1506
UNIVERSITÀ
DEGLI STUDI
DI URBINO
CARLO BO

UNIVERSITÀ DEGLI STUDI DI URBINO
"CARLO BO"
DIPARTIMENTO DI SCIENZE BIOMOLECOLARI

Corso di dottorato di Ricerca in:
Scienze della vita, Salute e Biotecnologie
Ciclo XXIX

Molecular identification and functional characterization of mitochondrial SVCT2 in leukemic cells and in the skeletal muscle.

SSD: BIO/14

RELATORE: Chiar.mo Prof.
Orazio Cantoni

DOTTORANDA: Dott.ssa
Maddalena Scotti

ANNO ACCADEMICO 2015/2016

INDEX

INTRODUCTION

1. VITAMIN C

Vitamin C (L-Ascorbic acid, AA) is a small water soluble molecule derived from glucose, involved in the first line antioxidant defense against oxidative stress, with the ability to prevent the damage induced on various biomolecules and subcellular compartments. AA can be de-protonated to ascorbate (Figure 1). Indeed, depending on the pH, AA may lose the hydrogen ions attached to either one of the two ionizable groups located at carbons 2' and 3', generating ascorbate mono-anion and di-anion [1]. The oxidation of AA is a reversible reaction; dehydroascorbate (DHA) can be converted back to AA by either GSH-dependent dehydroascorbate-reductase (transfer of 2 electrons) or NADH-dependent semi-dehydroascorbate-reductase (transfer of an electron). DHA is unstable at physiological pH and has a half-life of 5-15 minutes at 37° C [2].

Plants and many animals synthesize AA through different biosynthesis pathways. However, teleost fishes, some passeriform birds, guinea pigs, and non-human/human primates have lost the ability to synthesize AA, since they are deficient in L-gulonolactone oxidase. In humans, this enzyme is highly mutated and the gene encoding the protein is referred to as a pseudogene. For this reason, these species require AA from the diet [3]. In humans, the AA plasma concentration is maintained between 40 and 60 μM, and any excess is eliminated by the kidneys [4]. DHA concentrations in biological fluids are normally below 2 μM [5].

Scurvy was once a devastating illness in naval voyagers and for those who had little access to fresh fruits and vegetables [6]. Death typically occurred after several months of vitamin C deprivation and was characterized by the degeneration of almost every organ except the brain.Numerous biochemical, clinical, and epidemiological studies described the beneficial effects of vitamin C in chronic pathologies, in particular cardiovascular diseases, cataracts and cancer [7, 8]. The intake of nutrients rich in AA appears to be important for the prevention of cancer development [9-11], and the AA plasma concentration are in general inversely correlated with the risk of cancer [7, 12]. The recommended daily dose of vitamin C, necessary to maintain normal levels of the vitamin in plasma and tissues, is 75-125 mg [6]. AA is required to maintain the activity of a wide range of enzymes, to promote the biosynthesis of collagen, norepinephrine and carnitine and the catabolism of tyrosine [13]. In all these functions, the role of the vitamin C is to provide electrons to keep prosthetic metal ions (Fe^{2+} and Cu^{2+}) in their reduced forms. It is important to identify the role of vitamin C also as a cofactor for the regulation of the redox balance, and for its potential beneficial effects in the treatment of chronic degenerative diseases, autoimmune diseases and cancer [3].

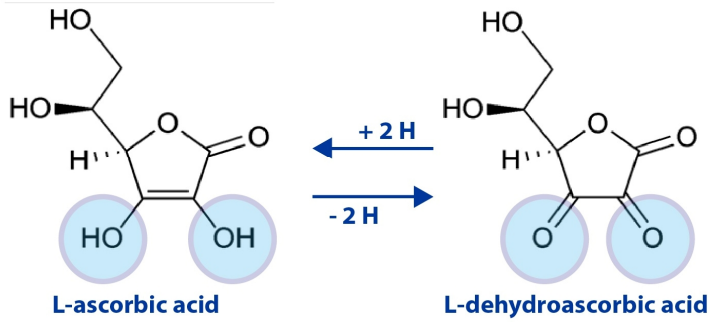

Figure 1. Structure and redox states of vitamin C

2. VITAMIN C TRANSPORTERS

AA levels are remarkably different in different tissues and the highest concentrations are reached in the adrenal glands, pituitary, lens, brain and liver [14]. The skeletal muscle contains lower amounts of AA, about 3-4 mg per 100 grams of tissue, corresponding to 70% of the total amount of vitamin C present in the body [14].

Several studies have shown that DHA can be taken up by the cells *via* a facilitated diffusion mechanism associated with the immediate intracellular reduction back to AA. This mechanism has been described in different cell types, including neutrophils [15], endothelial cells [16], astrocytes [17] and hepatocytes [18]. It has also been shown that DHA can be transported and reduced in the lumen of the endoplasmic reticulum [19, 20]. DHA, because of its similarity with glucose is transported into the cells by the hexose

transporters belonging to the family of GLUTs, in particular GLUT1, GLUT3 and GLUT4 [5], characterized by a low affinity / high capacity (Figure 3).

AA is instead taken up by the cells with an active mechanism, mediated by two distinct sodium-dependent transporters (SVCT1 and SVCT2), cloned for the first time in 1999 [21]. Both transporters are glycoproteins that belong to a family of nucleobase transporters, which includes general purine permease, bacterial xanthine transporter, uracil transporter and membrane-bound uracil permease. SVCT1 is encoded by a gene that belongs to the family of solute carriers, group 23A, member 1 (SLC23A1), with an open reading frame of 1797 bp, while the SLC23A2 gene with an open reading frame of 1952 bp encodes SVCT2. Homology among transcripts from different species (mouse, rat, pig and human) is about 90% for both mRNAs [22]. All the available information about the protein structure mainly derives from predictions based on primary amino acid sequence and Western blot analysis [23]. The overall amino acid identity of SVCT1 and SVCT2 is 65% in human and rat [21] and 60% in mouse [24]. Both are trans-membrane proteins; the predicted structure contains 12 membrane-spanning domains, with both the N- and C- termini located on the cytoplasmic side of the membrane. The extracellular loop between the 7 and 8 domains contains a series of conserved proline residues, which are needed for structure stability and transport efficiency [25] (Figure 2).

A

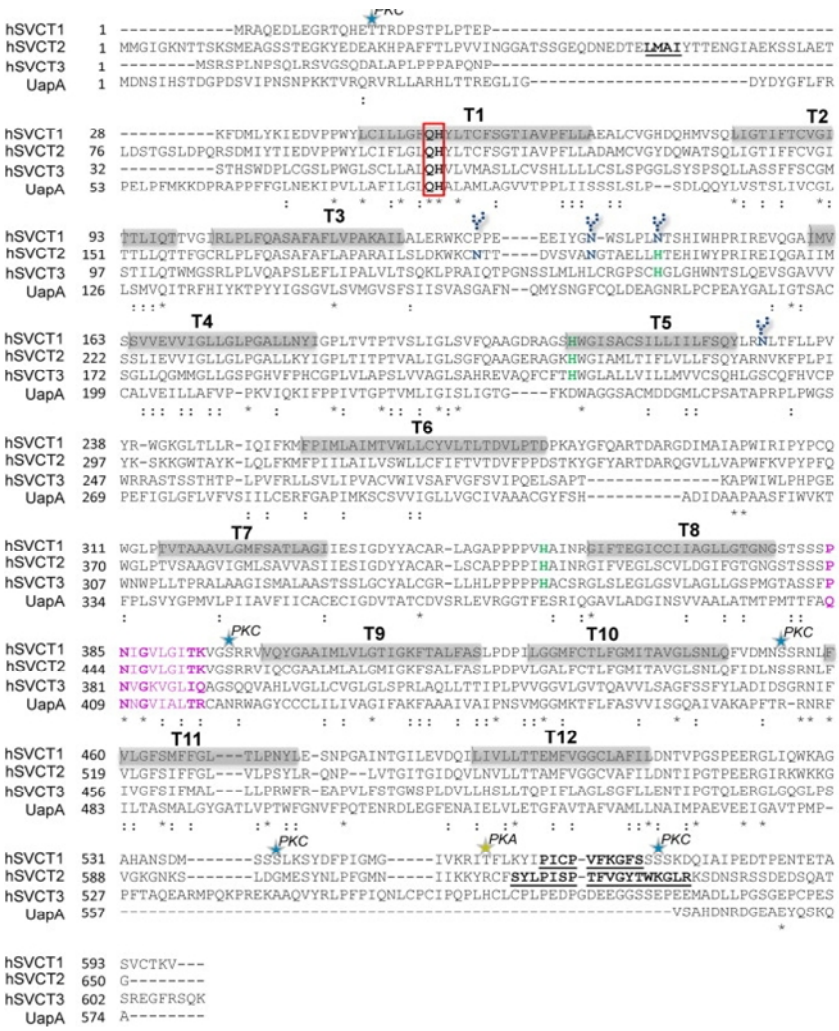
hSVCT1
hSVCT2
hSVCT3
UapA
T1
T2
T3
T4
T5
T6
T7
T8
T9
T10
T11
T12
PKC
PKA

B

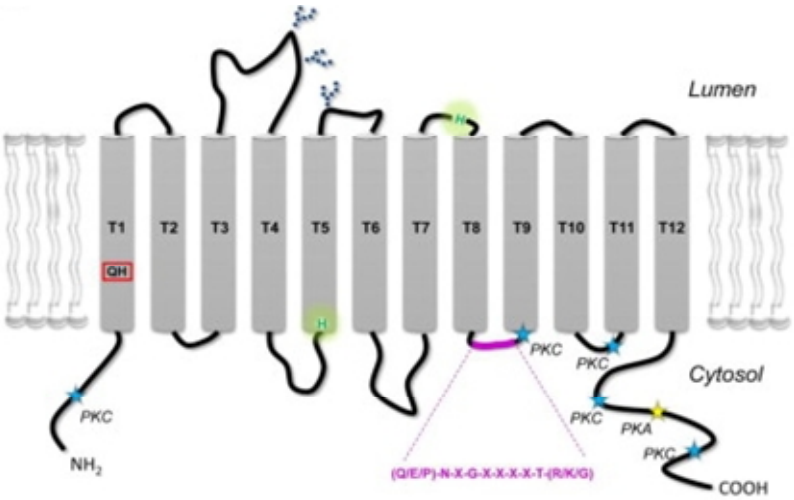
Lumen
Cytosol
T1
T2
T3
T4
T5
T6
T7
T8
T9
T10
T11
T12
QH
H
PKC
PKA
NH2
COOH
(Q/E/P)-N-X-G-X-X-X-X-T-(R/K/G)

Figure 2. Structure of SVCTs transporters. A) Alignment of human SVCT1, SVCT2 and SVCT3, and UapA amino acids. B) Membrane topology model of human SVCT1. The 12 putative transmembrane domains of human SVCT1 [26] are shaded in grey. These transmembrane domains are based on prediction algorithms for transmembrane topology. Relevant amino acid sequences in the N- and C-termini are underlined. Important histidine residues (green) and N-glycosylation sites (blue) of SVCT1 and SVCT2 are indicated. PKC and PKA sites of SVCT1 are labeled with asterisks. The highly conserved QH motif (red box) and signature motif (purple) are highlighted (Adapted from Burzle et al. [27]).

Non-functional splice variants have been identified for both human SVCT1 and SVCT2. In particular, the SVCT2 variant is a truncated protein, unable to transport AA, and possibly inhibiting this process through the wild type SVCT2 in tissues in which it is significantly expressed [28]. SVCT1 and SVCT2 are both Na^+-dependent transporters [29-31]. SVCT1 transports AA with a K_m of approximately 70 μM [32], although there are significant differences in the Km values (20–100 μM) detected in other studies performed in different cell types [21, 26]. The process is electrogenic and pH sensitive with an optimal pH at around 7.5. The transport of AA is 50–60% inhibited at pH 5.5 [26, 32]. SVCT2 has an apparent transport K_m of approximately 15 μM.SVCT1 and SVCT2 cotransport Na^+ and AA with a 2:1 stoichiometry down the electrochemical Na^+-gradient, with a binding order of Na^+, AA, and then Na^+[31, 32]. The

transport is electrogenic and the Hill coefficient for Na^+ is nearly 2 [21, 26]. Studies by Godoy et al. [31] revealed that the uptake of AA is more than 90% decreased in the absence of extracellular Na^+. Interestingly, SVCT2 was also shown to be Ca^{2+} and Mg^{2+}-dependent. The Authors suggested that, in the absence of Ca^{2+} and Mg^{2+}, SVCT2 is driven into an inactive state. Furthermore, they proposed that at low Na^+ concentrations (<20 mM) SVCT2 presents a low affinity conformation, whereas two high affinity conformations are observed when Na^+ concentrations are increased, and cooperativity of Na^+ is mediated by AA (Figure 3). Human SVCT1 is expressed in epithelial tissues, as the intestine, lung, liver, kidney and skin, and therefore contributes to the maintenance of whole-body AA levels. Human SVCT2 is instead more widely distributed (e.g. brain, lung, liver, skin, spleen, muscle, adrenal, eye, prostate and testis), and appears of pivotal importance for the protection of the cells against oxidative stress conditions [21, 26, 33, 34].

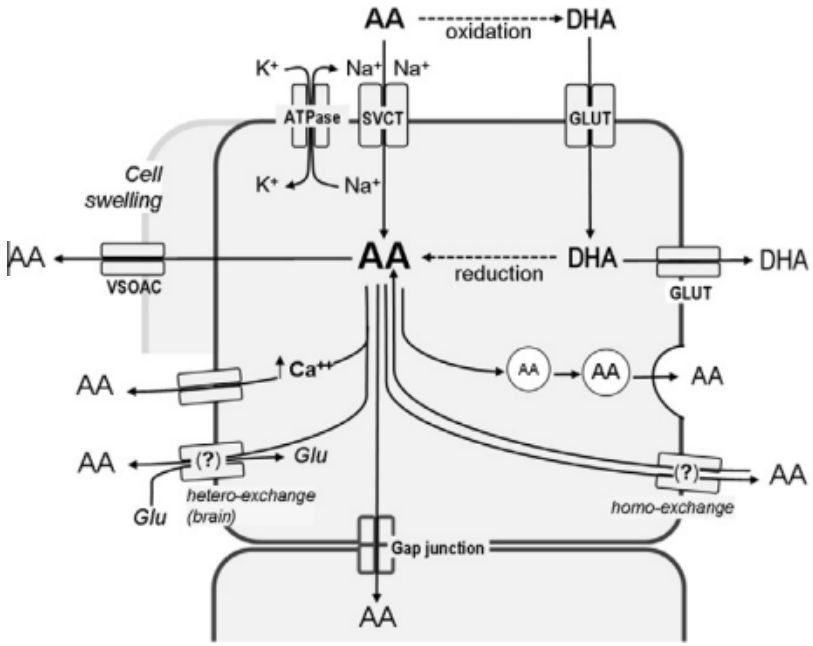

Figure 3. Vitamin C transport through the cell membrane [35]

3- VITAMIN C AND MITOCHONDRIA

Mitochondria are organelles found almost ubiquitously in eukaryotes. They are the location of a number of vitally important metabolic pathways, including the Krebs cycle, fatty acid oxidation, and lipid and cholesterol synthesis. One of its functions is the production of ATP, a versatile carrier of energy, in the respiratory chain/oxidative phosphorylation system. $NADH+H^+$ and $FADH_2$, produced by glycolysis, Krebs cycle and β-oxidation of fatty acids, are oxidized by the respiratory chain transferring electrons from these precursors to O_2. Incomplete reduction of oxygen occurs by electron leakage from Complex I (C-I) and Complex III (C-III), perhaps also from Complex IV (CIV). The resulting superoxide anion(O_2^-), is the source of other reactive intermediates, H_2O_2 and $HO^{\cdot}$. These three molecules, which represent endogenous oxidotoxins, are normally referred to as reactive oxygen species (ROS). They can be detoxified by the antioxidant defense system that includes superoxide dismutase (SOD), glutathione redox cycle, catalase and melatonin [36]. According to the chemiosmotic hypothesis [37], the free energy made available in the course of sequential electron transfer is used by C-I, C-III and C-IV to pump protons from the matrix to the inter-membrane space. This results in a proton gradient ($\Delta\mu_H^+$) over the mitochondrial inner membrane. This proton gradient is a source of free energy that is dissipated when protons enter the inner mitochondrial membrane *via* the ATP synthase. During this process,

ADP is phosphorylated to ATP, a high energy molecule consumed by many enzymes and numerous cellular processes [37]. Consequently, there is considerable interest in developing a basic understanding of how mitochondria function and how changes in variables such as levels of ROS, membrane potential, calcium or ATP concentrations may alter mitochondrial metabolism.

Since AA and its oxidized products are charged and water-soluble molecules, transporters are crucial to keep its concentrations optimal in the mitochondria. Although the first report on mitochondrial AA/DHA transport was published more than 30 years ago [38], many details of the transport were more clearly characterized in the last few years. The previous findings that vitamin C can enter plant mitochondria as DHA [23] were confirmed by Golde and co-workers [39] in animal cells. The mechanism whereby the vitamin is taken up by the mitochondria has been attributed for a long time to DHA transport for at least two separate reasons: i) hexose transporters are expressed in mitochondria [38-40], despite the lack of an apparent role of glucose in mitochondrial metabolism; ii) a high capacity transport is expected to be advantageous under conditions of extensive mitochondrial formation of ROS. Along the same lines, the possibility of a mitochondrial AA transport has been considered unlikely because of the high affinity of SVCTs, allowing the full expression of their activity at AA concentrations remarkably lower than those detected in the cytosol of many cell types *in vivo* [41, 42].

While this consideration deserves further discussion, there are two additional reasons arguing against a role of SVCTs in mitochondrial AA transport. The first one is based on the well- established Na^+-dependence of these transporters [21], the activity of which does not appear compatible with the concentrations of the cation in the intracellular fluids. The second reason against the mitochondrial location (and function) of SVCT2 is based on its Ca^{2+}-requirements for the expression of maximal activity [31]. Under resting conditions, there is an about four orders of magnitude difference in Ca^{2+} concentrations between the extra and intracellular compartments, with the possibility of a transient increase upon stimulation [43], however leading to Ca^{2+} concentrations still remarkably lower than those found in the extracellular milieu. Despite these observations and logical considerations, however, we recently provided evidence for the presence of SVTC2 immunoreactivity in U937 cell mitochondria [44]. Exposure of these cells to AA was associated with the mitochondrial accumulation of even low concentrations of the vitamin. These results were later on confirmed in HEK-293 cells by other investigators, that also provided kinetic information qualifying the mitochondrial SVCT2 as a low affinity transporter, due to the low intracellular Na^+concentrations [45].

4- AIM OF THE THESIS

The study described in this thesis represents a part of a research project developed in the section of Pharmacology, of the Department of Biomolecular Sciences, University of Urbino, aimed at the definition of vitamin C uptake mechanisms in the mitochondria of mammalian cells. Pioneer studies performed in this laboratory demonstrated the expression and functional activity of a mitochondrial SVCT2 in human promonocytic leukemic cells (U937) [44].The present study was performed with the aim of gathering more information on this transporter. In particular, I was interested in the characterization of the transport kinetics parameters of mitochondrial SVCT2. Furthermore, having previously shown that the expression of this transporter is permissive for the mitochondrial accumulation of large amounts of the vitamin, it was also important to determine the impact of this response in specific toxicity paradigms. A final point of interest was on the characterization of mitochondrial SVCT2 expression and activity during the differentiation process of U937 cells to monocytes. The second focus of this thesis was on the skeletal muscle. Since I was aware of the difficulties encountered by many investigators during the isolation of mitochondria from this tissue, however, I decided to first approach the issue under investigation in myotubes differentiated *in vitro* from C2C12 myoblasts to then move to the mouse *tibialis anterior* muscle tissue.

MATERIALS AND METHODS

1. Cell culture and treatment conditions.

U937 human myeloid leukemia cells and Raw 264.7 murine macrophages were cultured in RPMI 1640 medium (Sigma-Aldrich) supplemented with 10% heat-inactivated FBS (Euroclone, CelbioBiotecnologie, Milan, Italy), penicillin (100 units/ml) and streptomycin (100 µg/ml) (Euroclone). The cells were grown at 37°C in T-75 tissue culture flasks (Corning, Corning, NY) gassed with an atmosphere of 95% air-5% CO_2.

The undifferentiated U937 (U-U937) were differentiated to monocytes (D-U937) by a 4-day growth in culture medium supplemented with 1.3% dimethyl sulfoxide (DMSO), as previous described [52].

C2C12 mouse adherent myoblasts (Mb) were grown in DMEM medium (Sigma-Aldrich) supplemented with 10% heat inactivated FBS (Euroclone, CelbioBiotecnologie, Milan, Italy), 2 mM l-glutamine and penicillin (100 units/ml) and streptomycin (100 µg/ml) (Euroclone). The cells were grown at 37°C in a 5% CO_2 humidified atmosphere. Upon 70-80% confluency, C2C12 Mb were triggered to differentiate by changing the growth medium to DMEM containing 1% heat inactivated FBS.

Cells were exposed for 5-10 min to AA or ^{14}C-AA (specific activity 5.35 mCi/mmol) in Extracellular Buffer, EB (15 mMHepes, 135 mMNaCl, 5 mMKCl, 1.8 mM CaCl2, 0.8 mM MgCl2, pH 7.4) in the presence of 0.1 mM DTT. A 10 mM AA stock solution was prepared immediately before use.Stability of AA (30 µM) in the above EB was

assessed by monitoring the absorbance at 267 nm for 90 min (ε267=14,600 M-1 cm-1). In selected experiments, NaCl was replaced with choline-chloride.

2. Purification of mitochondria and subcellular fractionation.

The cells were processed to obtain the following sub-cellular fractions: crude mitochondria (Mc), pure mitochondria (Mp), plasma membranes (PM), endoplasmic reticulum (ER) as described in ref. [53]. Briefly, cells were washed in PBS twice, resuspended in cold (4°C) homogenization buffer (HB: 225 mM mannitol, 75 mM sucrose, 0.1 mM EGTA, protease inhibitor cocktail, 5 mM Tris-HCl pH 7.4) and homogenized using a glass potter in ice-bath. The efficiency of homogenization was monitored using trypan blue and stopped when 90% of the cells were disintegrated. The homogenate was centrifuged at 1000x*g* for 20 min at 4°C and the supernatant (S1) collected for the final centrifugation. The pellet was re-homogenized and the supernatant (S2) added to S1 and centrifuged at 20000x*g* for 30 min at 4°C. The pellet corresponding to crude mitochondria (Mc) was washed with HB. The supernatant was centrifuged at 95000x*g* for 60 min to obtain the ER fraction (pellet) and the cytosol (C) (supernatant). The pellet corresponding to Mc was resuspended in MRB buffer (250mM mannitol, 5mM HEPES, 0.5mM EGTA, pH7.4) and separated by centrifugation at 95000xg for 2 hours on 30% Percoll gradient. The lower density band, corresponding to the pure

mitochondrial fraction (Mp), was collected and washed two times in MRB at 6300 x *g* for 20 min [53].

The mitochondria from skeletal muscle tissues were obtained by differential centrifugation, following the protocol of Frezza et al. [54]. Muscles were taken from the back legs of the mice (*tibialis anterior*), isolated from the bone and turned away of fat, tendons and connective tissue. Subsequently, the tissue was chopped with a scalpel, scissors and tweezers, using as support a steel plate on ice. The chopped muscle tissue was then washed 3 times with cold PBS + 10 mM EDTA, 0.5 mM DTT + 5.77 mM ATP using a metal strainer. The pieces were re-suspended in cold PBS + 10 mM EDTA + 0.5% trypsin, vortexed and left on ice for 30 minutes. The chopped tissue was centrifuged at 1000 rpm for 5 minutes at 4 ° C. The pellet was re-suspended in IBM1 (1M sucrose, 1M Tris/HCl, 1M KCl, 1M EDTA, 10% BSA, pH 7.4) + 1.8 mM ATP (ratio 1: 5 or 1:10) and homogenized using a Potter homogenizer provided with glass Teflon pestle connected by a steel pole to an electric motor. All these steps were performed on ice. Total homogenate aliquots were taken for Western Blot analysis. The remaining homogenate was centrifuged at 1800 rpm for 10 minutes at 4° C. The supernatant (S1) was transferred to a centrifuge tube suitable to JA20 rotor, while the pellet was re-suspended in IBM1 and re-homogenate as described above obtaining S2. S1 and S2 were combined and centrifuged at 8000 rpm for 10 minutes at 4° C. After removal of the supernatant,

the pellet corresponding to the mitochondria was re-suspended in 10 ml cold IBM2 (1M sucrose, 0.1 M EGTA/Tris, 1 M tris/HCl, pH 7.4) and centrifuged again at 8000 rpm for 10 minutes at 4° C. The pellet corresponding to Mc was re-suspended in MRB buffer (250mM mannitol, 5mM HEPES, 0.5mM EGTA, pH7.4) and separated by centrifugation at 95000xg for 2 hours on 30% Percoll gradient. The lower density band, corresponding to the pure mitochondrial fraction (Mp), was collected and washed two times in MRB at 6300 x *g* for 20 min [53].

3. Uptake of ^{14}C AA in isolated mitochondria

The isolated mitochondria were exposed to ^{14}C-AA in Incubation Buffer (IB, 15 mM Hepes-Na; 15 mMNaCl, 120 mMKCl, 1 mM MgCl2, pH 7.6) containing 0.1 mM DTT. After the treatments, the samples were centrifuged (10000 rpm for 5 minutes at 4 ° C), the incubation buffer removed and the cells washed twice with 1 mM AA + IB + cold 1 mM DTT. The cells were then lysed with NaOH 0.5 N and the samples transferred to the vials. After the addition of 4 ml of scintillating liquid (Universal LSC-cocktail Ultima Gold), the samples were placed in the scintillator (analyzer in liquid phase Tri-carb 2100TR-model) for the determination of associated radioactivity.

4. Western blot (WB) assay.

Equal amounts (30 μg) of sub-cellular fractions and whole cell lysates were resolved in 12.5 or 15% sodium dodecyl sulphate polyacrylamide gel and electrotransferred to polyvinyldienedifluoride membranes (PVDF). Western blot analysis was performed using antibodies against SVCT2, cytochrome c, calnexin, GLUT3 and actin. Details on Western blotting apparatus and conditions are reported elsewhere [56]. Antibodies against cytochrome c, calnexin and GLUT3 were used to assess and the purity of the fractions.

5. Reverse transcriptase-polymerase chain reaction (RT-PCR).

1 μg of total RNA, purified with TRIzol protocol, was pre-treated with Dnase I and used for cDNA synthesis with the SMARTScribe Reverse Transcriptase. The following primers were used to analyze the expression of: SVCT1: For 5'-GCCCCTGAACACCTCTCATA-3' and Rev 5'-ATGGCCAGCATGATAGGAAA-3'; SVCT2: For 5'-TTCTGTGTGGGAATCACTAC-3' and Rev 5'-ACCAGAGAGGCCAATTAGGG-3'. Amplification of GAPDH was used for internal control. Amplification products were examined by electrophoresis on 1.5-2% agarose gels and visualized with ethidium bromide.

6. Transmission Electron Microscopy (TEM) analysis.

Cells were fixed with 2.5% glutaraldehyde in 0.1 M phosphate buffer for 15 min. Pellets were further processed as reported by Burattini et al. [57]. The analyses were performed in Prof. Falcieri's lab, in the Department of Biomolecular Sciences, Università degli Studi di Urbino.

7. Immunolocalization by confocal microscopy.

Cells were incubated for 20 min with 50 nM MitoTraker Red (Molecular Probes, Europe, Leiden, The Netherlands) in 2 ml of PBS in 35-mm tissue culture dishes containing an uncoated coverslip. The cells were then fixed for 1 min with 4% paraformaldehyde, RT, washed with PBS (8 g/l NaCl, 1.15 g/l Na_2HPO_4, 0.2 g/l KH_2PO_4, and 0.2 g/l KCl, pH 7.4), permeabilized with 0.1% Triton X-100 in PBS and then blocked in PBS containing BSA (2% w/v) for 30 min. The cells were subsequently incubated with goat polyclonal anti-SVCT2 antibody (1:100 in PBS containing 2% BSA), stored for 18 h at 4°C, washed and then exposed to FITC-conjugated secondary antibody diluted 1/100 in PBS for 2h in the dark. The digital images were acquired on a Leica TCS-SP5 CSLM mounted on a Leica DMI 6000 CS inverted microscope (Leica Microsystems CMS GmbH, Mannheim, Germany) at 512x512 using 63.0 x 1.4 oil objective (HCX PL APO 63.0 x 1.40 OIL UV) and with appropriate excitation / detection

settings (FITC argon laser 488 nm / 500-535 nm emission filter; MitoTracker Red HeNe laser 543 nm / 555-610 nm emission filter).Images and degree of co-localization were analyzed by the Leica Application Suite Advanced Fluorescence (LASAF) and JACoP, a plugin for the ImageJ Software (Wayne Rasband, Bethesda, MA). We used Pearson's coefficient as the parameter to measure co-localization in our samples. These analyses were performed in Prof. Falcieri's lab.

8. Cytotoxicity Assay

After treatments with peroxynitrite, the number of viable cells was estimated with the trypan blue exclusion assay. Briefly, an aliquot of the cell suspension was diluted 1:2 (v/v) with 0.4% trypan blue and the viable cells (i.e., those excluding trypan blue) were counted with a hemocytometer.

9. MitoSOX red oxidation

Cells were first exposed for 15 min (37°C) to 5 µM MitoSOX red, washed two times with saline A and finally treated as detailed in the legend to the figures. After treatments, the cells were washed three times and fluorescence images were captured with a BX-51 microscope (Olympus, Milan, Italy), equipped with a SPOT-RT camera unit (Diagnostic Instruments, Delta Sistemi, Rome, Italy) using an Olympus LCAch 40 x/0.55 objective lens. The excitation and emission

wavelengths were 510 and 580 nm with a 5-nm slit width for both emission and excitation. Images were collected with exposure times of 100-400 ms, digitally acquired and processed for fluorescence determination at the single cell level on a personal computer using Scion Image software (Scion Corp., Frederick, MD). Mean fluorescence values were determined by averaging the fluorescence values of at least 50 cells/ treatment condition/experiment.

10. Alkaline-halo assay

DNA single-strand breakage was determined using the alkaline halo assay developed in our laboratory [58]. It is important to keep in mind that, although we refer to DNA strand scission throughout the text, the DNA nicks measured by this technique under alkaline conditions may in fact include alkali labile sites in addition to direct strand breaks. Details on the alkaline halo assay and processing of fluorescence images and on the calculation of the experimental results are also given in Ref. [58]. DNA single-strand breakage was quantified by calculating the nuclear spreading factor value, representing the ratio between the area of the halo (obtained by subtracting the area of the nucleus from the total area, nucleus + halo) and that of the nucleus, from 50 to 75 randomly selected cells/experiment/treatment condition. Results are expressed as relative nuclear spreading factor values calculated by subtracting the

nuclear spreading factor values of control cells from those of treated cells.

11. Kinetic calculations

The transport kinetic parameters were calculated by using the Michaelis-Menten equation and the linear transformation of Eadie-Hofstee. Kinetic parameters were estimated from the fitted curves using the Graph Pad Prism software designed for nonlinear regression analysis.

12. Statistical analysis

The results are expressed as means ± SD. Statistical differences were analyzed by one-way ANOVA followed by Dunnett's test for multiple comparison or two-way ANOVA followed by Bonferroni's test for multiple comparison. A value of $P < 0.05$ was considered significant.

RESULTS AND DISCUSSION

1. ASCORBIC ACIDTRANSPORT IN U937 CELLS

1.1 Kinetic characterization of mitochondrial SVCT2 in U937 cells.

The expression of functional SVCT2 in U937 cells mitochondria was recently demonstrated in our laboratory [44]. In particular, we found that a 10 min exposure to 10 μM AA is associated with the accumulation of an about 150 μM concentration of the vitamin in the cytosol and with a 10 mM concentration in mitochondria. This observation suggests the involvement of a high affinity transport of AA in mitochondria. In our initial experiments, we decided to provide more data further demonstrating the mitochondrial localization of SVCT2.

Figure 4A and B provides evidence of a punctuate fluorescence response evoked by a mitochondrial probe (MitoTraker red) in U937 cells. A similar subcellular distribution of the fluorescence was observed in cultures supplemented with an anti-SVCT2 antibody. The mitochondrial expression of SVCT2 was confirmed by appropriate co-localization analyses (Figure 4C-E). Coherent information is provided by the identification of the same bands in immunoblot experiments using anti-SVCT2 antibodies and mitochondrial preparations obtained with two different isolation procedures (Figure 4F). Finally, the mitochondrial localization of SVCT2 is also consistent with the results obtained in immunoblotting experiments using markers for the

nuclear, mitochondrial, plasma membrane, endoplasmic reticulum and cytosol enriched fractions (Figure 4G).

We then moved to experiments aimed at the assessment of the kinetic characteristics of U937 cell mitochondrial SVCT2. As previously indicated, this transporter is expected to display low substrate affinity, due to the cytosolic milieu, different in ionic composition from extracellular fluids [31]. On the other hand, the very high accumulation of AA in mitochondria might represent an indication of the expression of a high affinity transport of the vitamin.

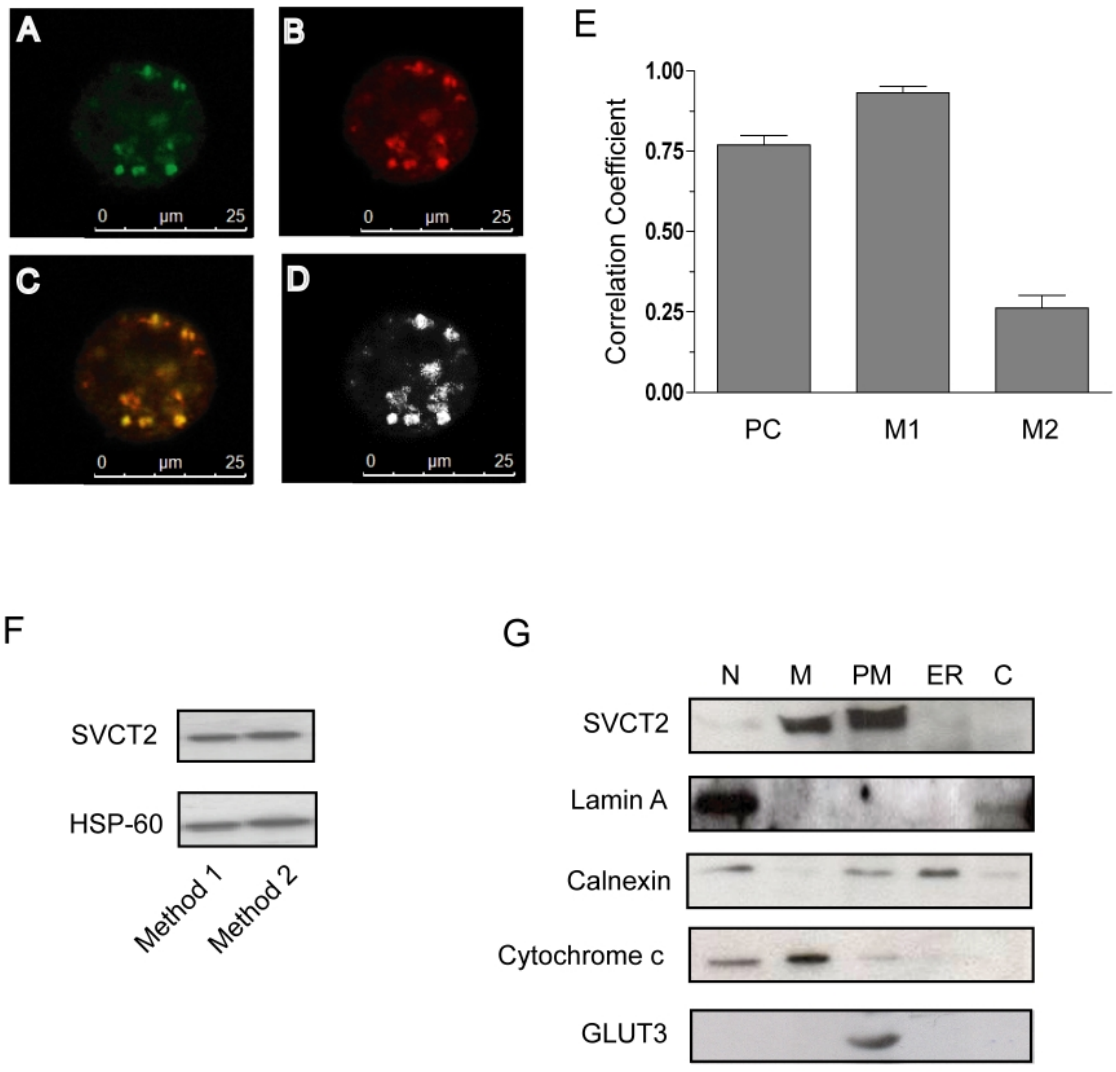

Figure 4. Subcellular localization of SVCT2 in U937 cells. (A–E) Co-localization of anti-SVCT2 immunoreactivity with a mitochondrial fluorescent probe (MitoTracker Red) in U937 cells. Representative fluorescence images of cells double stained for SVCT2 (green, A) and mitochondria (red, B). In the merged images, the regions containing both MitoTracker Red and FITC fluorescence appear yellow (C). (D) Colocalisation analysis and quantification. (E) The Pearson's (PC) and Manders' (M1 and M2) overlap coefficients represented as the average of ten individual cells. (F) Mitochondrial fractions obtained from two different lots of untreated U937 cells were processed for Western blot analysis using antibodies against

SVCT2. Blots were re-probed for HSP-60. Mitochondria were isolated by a differential centrifugation procedure (Method 1) or by sucrose gradient centrifugation (Method 2). (G) U937 cells were homogenized and fractionated by differential centrifugation and the different fractions (N: nuclear fraction; M: mitochondria; ER: endoplasmic reticulum; PM: plasma membranes enriched fraction; C: cytoplasmic fraction) were processed for Western blot analysis. Blots shown are representative of 2 separate experiments with similar outcomes [59].

We initially performed a time course analysis of AA(30 μM) uptake in isolated mitochondria (MB: 5 mM HEPES, 210 mM mannitol, 70 mM sucrose, 1 mM Na-EGTA, pH 7.4)and found that these organelles take up AA at a constant rate of 0.48± 0.055 nmol/mg prot/min for at least 5 min (Figure 5A). We then exposed mitochondria for 3 min to increasing concentrations of AA and obtained a response well described by a hyperbolic curve saturating at 60 μM AA (Figure 5B). Analysis of the transport data by the Eadie–Hofstee method (Figure 5C) produced a straight line (r^2 = 0.95), consistent with the presence of a functional component, allowing the calculation of an apparent Km of 26.96 ± 1.46 μM and a Vmax of 1.24± 0.045 nmol/mg prot/min. It is interesting to note that similar experiments using a K^+-containing buffer (IB: 15 mM HEPES-Na, 15 mM NaCl, 120 mM KCl, 1 mM $MgCl_2$, pH 7.6) produced identical results (Figure 5D and E) with an even lower Km (22.40 ± 1.6 μM), despite the recent indication that K^+ may

in fact reduce the affinity of the mitochondrial AA transporter [45]. Results illustrated in Figure 5F provide evidence for a progressive loss of activity at descending pH values. We also performed experiments using intact Raw 264.7 cells, which only express SVCT2 (Figure 6A, inset a). The concentration–dependence for the accumulation of the vitamin is reported in the inset (b) to Figure 6A. Eadie-Hofstee analysis of this data produced a straight line (r^2 = 0.95), as previously shown for U937 cell mitochondria, allowing the calculation of a similar Km value (22.4 ± 1.66 μM). To draw a comparison, similar experiments were performed in intact U937 cells, which express both SVCT1 and 2 (Figure 6B, inset a). This experiments generated a hyperbolic dose-response curve (Figure 6B, inset b) that, when analyzed by the Eadie-Hofstee method (Figure 6B), revealed a non linear relationship that fits well with a model describing the involvement of two saturable transport systems for AA, with different affinities for the substrate; the higher affinity component had an apparent Km of 8.4 ± 0.76 μM and Vmax 0.11 ± 0.007 nmol/mg prot/min, whereas the lower affinity component had apparent Km and Vmax values of 85.5 ± 7.9 μM and 0.48 ± 0.03 nmol/mg prot/min, respectively. These Km values are in the expected range for SVCT2 and SVCT1 [60-62].An additional important similarity was found for the pH-dependent regulation of SVCT2-mediated AA transport. Our results obtained with intact Raw 264.7 cells (Figure 6C) are in keeping with the notion that SVCT2 activity is impaired at acid pH

[63]; a virtually superimposable curve was obtained in experiments performed with isolated mitochondria (Figure 5F).

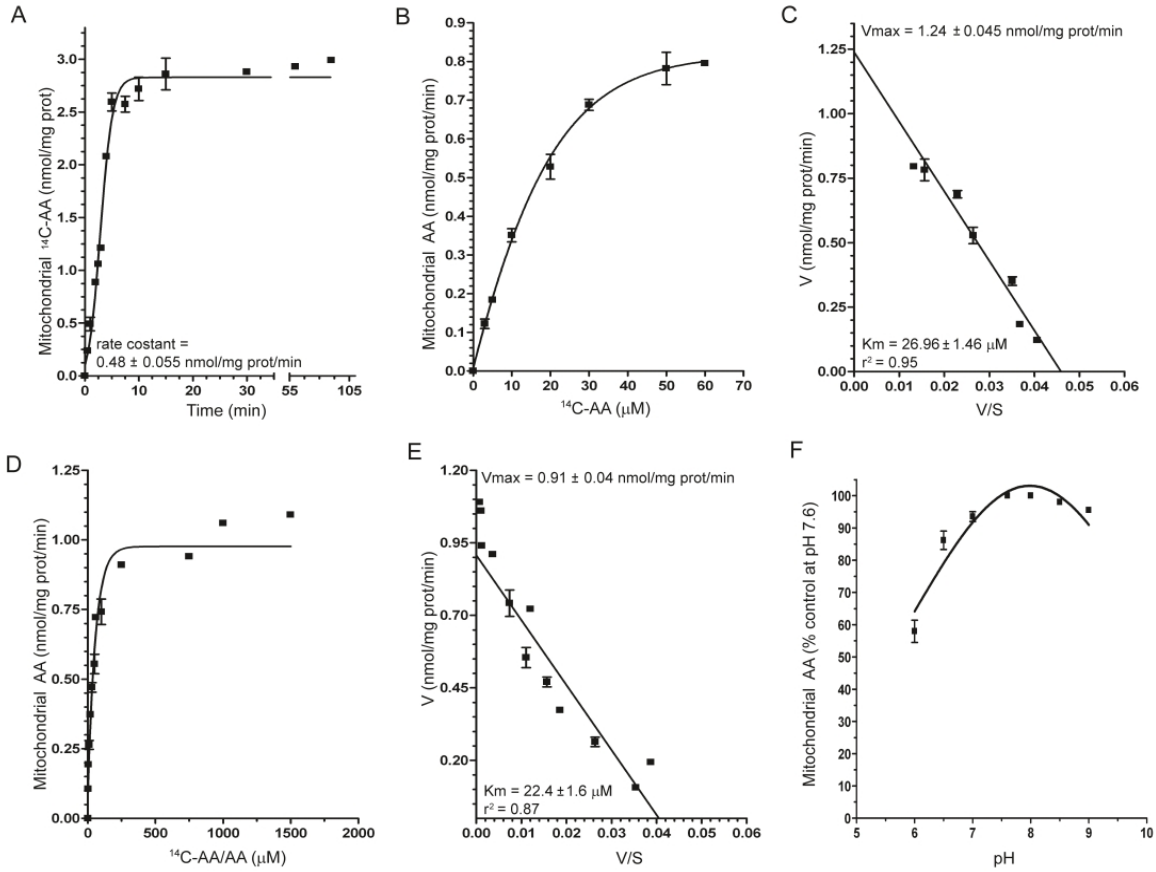

Figure 5. Kinetic properties of mitochondrial SVCT2 in U937 cells. (A) Time-dependence of AA accumulation in isolated mitochondria exposed to 30 μM ^{14}C-AA in MB. (B) AA content in isolated mitochondria exposed to 0–60 μM ^{14}C-AA in MB. (C) Eadie–Hofstee plot of the data in B. (D) AA content in isolated mitochondria exposed to 0–1.5 mM ^{14}C-AA/AA in IB. (E) Eadie–Hofstee plot of the data in D. (F) AA uptake in isolated mitochondria exposed to 30 μM AA at different pH values in IB [59].

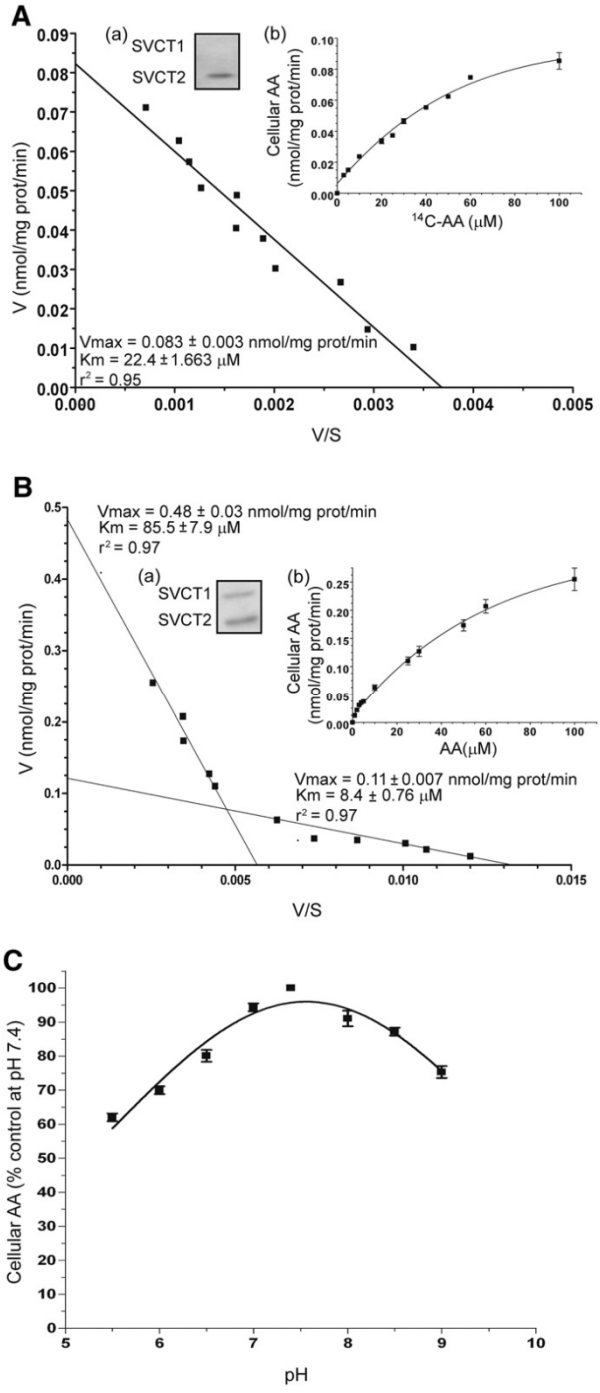

Figure 6. AA transport in Raw 264.7 and U937 cells. (A) Eadie – Hofstee plot of the concentration-response curve for AA transport in Raw 264.7 cells. Inset (a): Raw 264.7 cell lysates were processed for Western blot analysis using antibodies against SVCT1 and SVCT2. Inset (b): AA content in Raw 264.7 cells exposed to 0–100 μM ^{14}C-AA in EB. (B) Eadie–Hofstee plot of the concentration–response curve for AA transport in U937

cells. Inset (a): U937 cell lysates were processed for Western blot analysis using antibodies against SVCT1 and SVCT2. Inset (b): AA content in U937 cells exposed to 0–100 μM AA in EB. (C) AA uptake in Raw 264.7 cells exposed to 30 μM AA at different pH values in EB. Values are means, with standard deviations calculated from at least three separate experiments [59].

Plasma membrane SVCT2-mediated transport of AA is activated by high Na^+ concentrations, i.e., those normally detected in the extracellular milieu [30]. The Na^+-dependence of AA transport was therefore investigated in mitochondria isolated from U937 cells. The results illustrated in Figure 7A are from experiments in which MB was supplemented with 30 μM AA and increasing concentrations of Na^+. These results clearly establish the Na^+-dependent activation of the mitochondrial SVCT2 at surprisingly low concentrations of the cation. Indeed, mitochondrial uptake of AA increased linearly with increasing Na^+ concentrations, reaching a plateau at 1 mM, with a Na_{50} (the Na^+ concentration inducing a 50% of the AA maximal uptake rate) of 0.525 mM. We then performed similar experiments in which MB was replaced with IB. As indicated in Figure 7B, AA uptake was somewhat increased under these conditions but, most importantly, the plateau was reached once again at 1 mM Na^+. The sigmoidal curves outlined in Figure 7A and B are indicative of a cooperative mechanism, also emphasised by the Hill plot (insets to Figure 7Aand B) leading to a calculated nH values of 2.2 ± 0.1 and 2.0 ± 0.16,respectively.We

finally tested the Na^+-dependence for AA transport in Raw264.7 cells and obtained data in line with those previously reported in other studies [30].

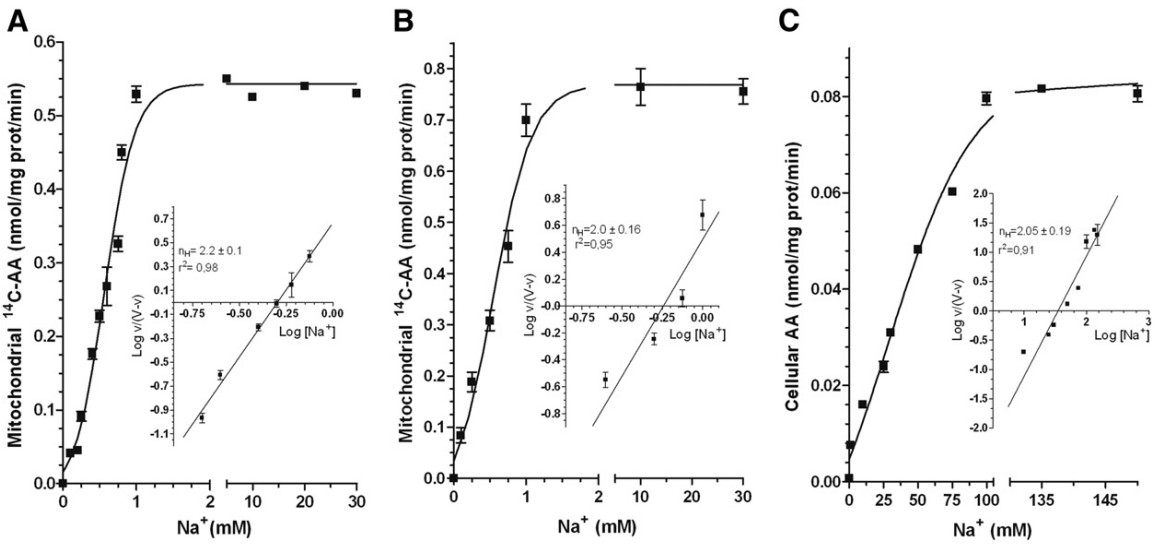

Figure 7. Na^+-dependence of AA transport in mitochondria isolated from U937 cells and in intact Raw 264.7 cells. (A) Effect of increasing Na^+ concentrations on ^{14}C-AA (30 μM) uptake in isolated U937 cell mitochondria bathed in MB. Inset: Hill plot of the data in A. (B) Effect of increasing Na+ concentrations on ^{14}C-AA (30 μM) uptake in isolated U937 cell mitochondria bathed in IB. Inset: Hill plot of the data in B. (C) Effect of increasing Na^+ concentrations on AA (30 μM) uptake in intact Raw 264.7 cells bathed in EB. Inset: Hill plot of the data in C. Values are means, with standard deviations calculated from at least three separate experiments [59].

Plasma membrane SVCT2–mediated transport of AA has an absolute requirement for Ca^{2+} and Mg^{2+}[31]. Coherently, omission of Ca^{2+} and $Mg^{2+}$from the extracellular milieu abolished AA (30 μM) transport in Raw 264.7 cells, whereas hardly any effect was obtained with the omission of either Ca^{2+} or Mg^{2+} alone (Figure 8A). Results obtained in U937 cells were somewhat different, as some residual AA transport activity was found in the absence of both cations (Figure 8A), most likely dependent on SVCT1 activity. These results are therefore different from those reported in Fig. 5B(using isolated mitochondria), in which AA transport studies were performed using a Ca^{2+}/Mg^{2+}-free buffer supplemented with EGTA(MB).Further studies revealed that AA transport in isolated mitochondria is not affected by removal of EGTA and is abolished by Na^{+} omission, regardless of the presence of EGTA. Moreover, AA transport rate in EGTA-free MB was insensitive to addition of Ca^{2+} (0.25 μM) and/or Mg^{2+} (2.5 mM) (Figure 8B). The Ca^{2+} and/or Mg^{2+} independence of AA transport in isolated mitochondria was also established in experiments in which MB was replaced with IB (not shown). These results therefore indicate that mitochondrial SVCT2-mediated AA transport is Ca^{2+} and Mg^{2+}-independent and is not further stimulated by increases in Ca^{2+} and/or Mg^{2+} concentrations.

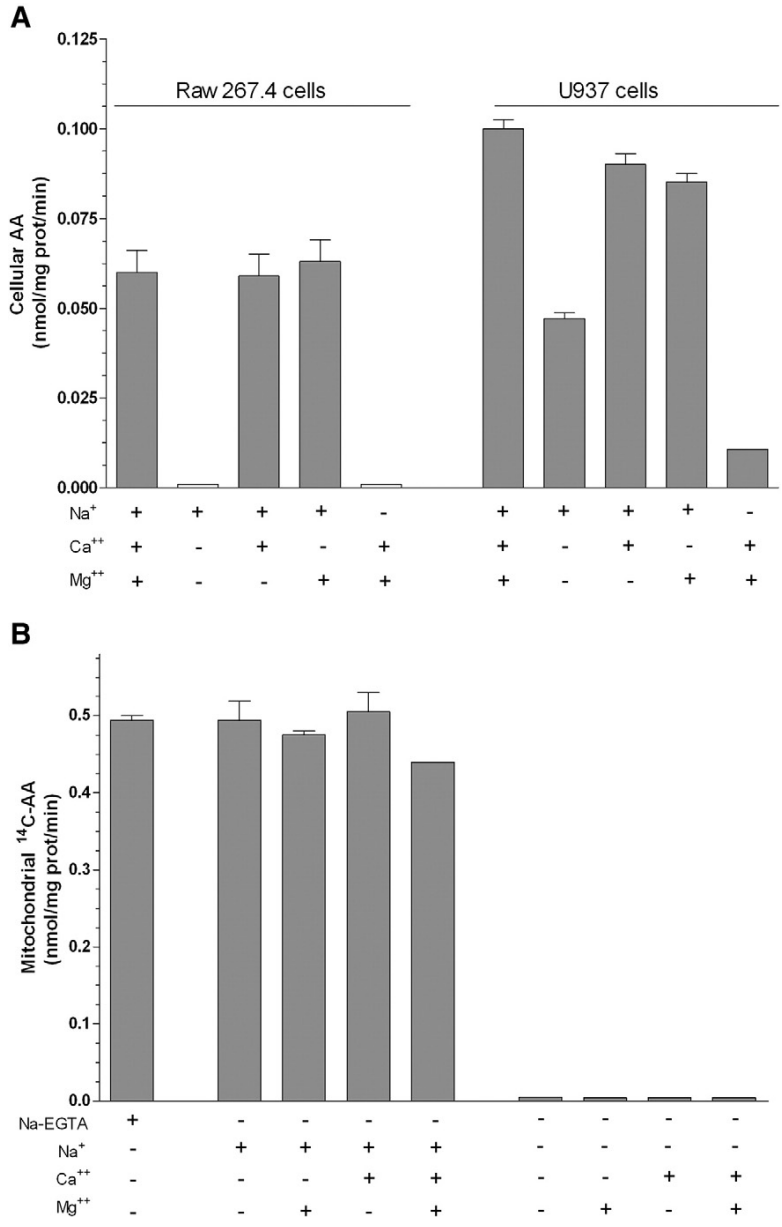

Figure 8. Ca^{2+} and/or Mg^{2+}-dependence of AA transport in intact Raw 264.7 cells, U937 cells and mitochondria isolated from U937 cells. (A) Raw 264.7 and U937 cells were exposed to ^{14}C-AA (30 μM) in EB manipulated as indicated in the figure. AA uptake was then determined. (B) Mitochondria isolated from U937 cells were exposed to ^{14}C-AA (30 μM) in MB manipulated as indicated in the figure and then analyzed for AA accumulation. Values are means, with standard deviations calculated from at least three separate experiments [59].

In conclusion, our work provides further evidence for the mitochondrial localization of SVCT2 in U937 cells and demonstrates that this transporter, because of the very low requirements for Na^+ and divalent cations, has an affinity comparable with that of the plasma membrane SVCT2[59]. These results imply that different cells types might accumulate AA in their mitochondria through both high and low affinity SVCT2.

The mitochondrial accumulation of AA has important implications in an array of events that take place in these organelles. For example, we recently found that a short-term pre-exposure to as low as 3 μM AA prevents the toxic effects mediated by prolonged exposure to arsenite [64]. Under these conditions, the metalloid selectively triggers the mitochondrial formation of superoxide/H_2O_2 and the ensuing mitochondrial permeability transition followed by delayed apoptotic death: the mitochondrial fraction of AA was found to prevent superoxide/H_2O_2 and the above downstream events.

In general, intra-mitochondrial AA is expected to display antioxidant properties associated with prevention of the deleterious effects mediated by a large variety of reactive species, including peroxides, hydroxyl radicals, superoxide (O_2^-), and peroxynitrite [47, 48]. Although cytoprotection may also be induced *via* additional mechanisms, growing experimental evidence documents an unexpected ability of intra-mitochondrial AA to promote opposite effects, in particular after exposure to otherwise inactive

concentrations of different oxidants [58, 68, 73]. These enhancing effects have nothing to do with extracellular $O_2^{-\cdot}$ generated by autoxidation of high concentrations of AA in solution, and are in fact mediated by the intracellular fraction of the vitamin *via* a mechanism saturating at low concentrations of AA [64, 74].

Given this premise, cellular and mitochondrial transport of AA is likely regulated by various independent pathways. Interestingly, we recently described [66] a mechanism limiting the activity of both the plasma membrane [65] and mitochondrial SVCT2 [59], controlled by DHA. Indeed, the combined treatment with AA and DHA leads to the same cellular and mitochondrial accumulation of the vitamin observed after treatment with DHA alone (Figure 9A and its inset). Thus, while cellular uptake of AA appears linked to a rapid transport of the vitamin in mitochondria, the results obtained with DHA alone, or combined with AA, are of more complex interpretation. More specifically, DHA is the species crossing the plasma membrane in both of these conditions [65] and it is unclear why, even at fairly high concentration (e.g., 30 μM), it is poorly taken up by the mitochondria, either directly or as DHA-derived AA. In order to address this issue, we investigated the rate of intracellular reduction of DHA. In these experiments, the cells were exposed for increasing time intervals to 30 μM AA, or DHA, and subsequently processed for the assessment of vitamin C accumulation, with or without DTT (10 mM) treatment of the lysates prior to HPLC analysis (Figure 9B). The

results are indicative of an immediate reduction of DHA back to AA, thereby leading to the straightforward conclusion that, under these conditions, direct mitochondrial uptake of DHA is limited by the poor substrate concentrations. Significant mitochondrial accumulation of AA was however detected in cells exposed to very high concentrations of DHA (Figure 9C), an observation consistent with the possibility of a direct mitochondrial uptake of the oxidized form of the vitamin. A comparison of the results obtained after exposure to AA or DHA provides evidence for an enormous difference in the mitochondrial accumulation of vitamin C associated with the two treatments. As an example, similar mitochondrial accumulation of vitamin C was measured in cells exposed to 10 µM AA or 300 µM DHA, i.e., under conditions in which the overall cellular accumulation of the vitamin was dramatically different (Figure 9C, inset).These results indicate that low extracellular concentrations of DHA are associated with rapid uptake and rapid reduction back to AA, so that direct mitochondrial uptake of DHA cannot take place at significant amounts. At increasing extracellular DHA concentrations, however, intracellular steady-state concentrations of DHA progressively increase, thereby enhancing the possibility of its mitochondrial uptake through hexose transporters. The DHA concentration-dependence for the mitochondrial accumulation of the vitamin in cells exposed to 30 µM AA is illustrated in Figure 9D.

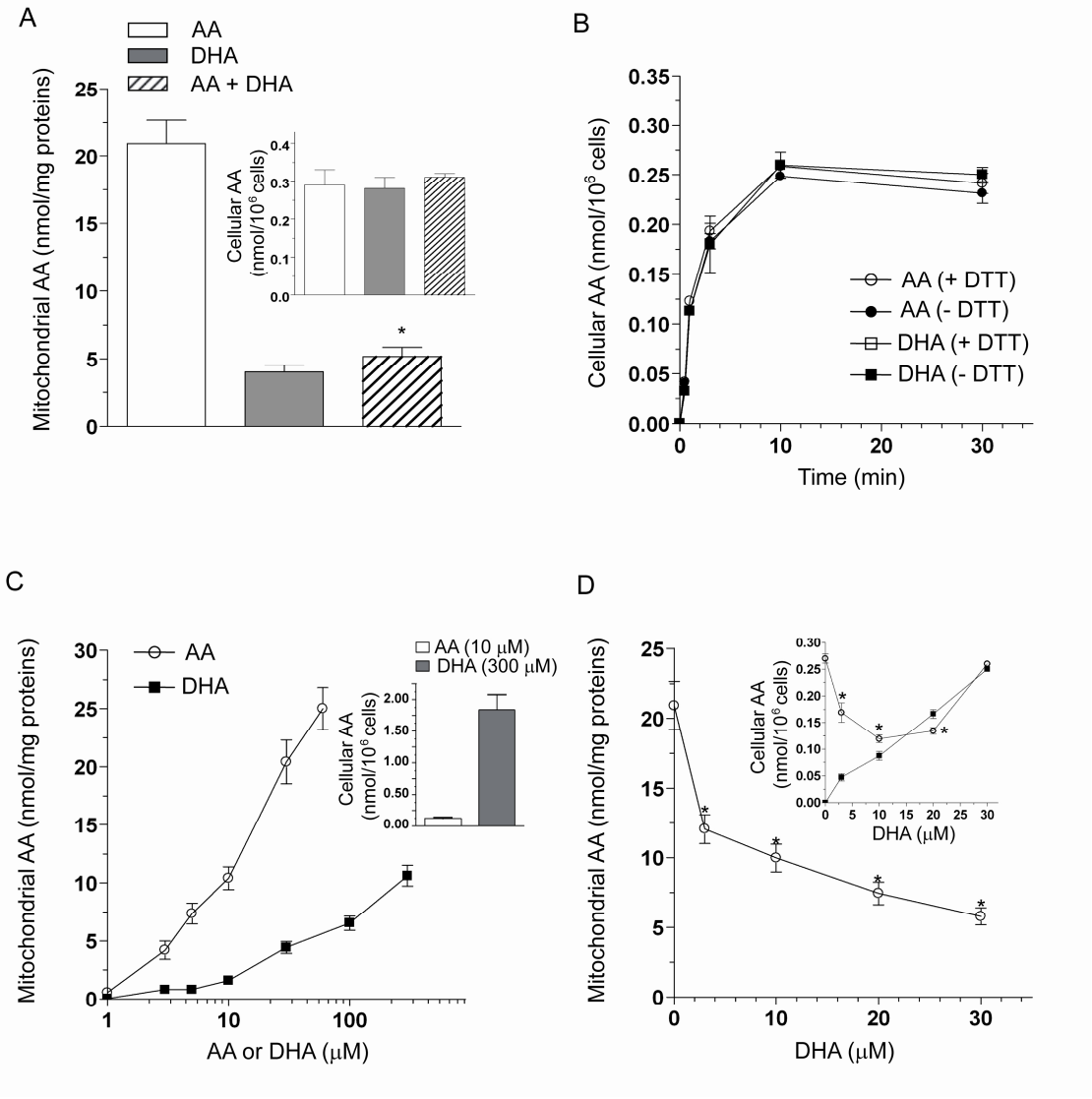
A
AA
DHA
AA + DHA
Mitochondrial AA (nmol/mg proteins)
Cellular AA (nmol/10^6 cells)
B
Cellular AA (nmol/10^6 cells)
AA (+ DTT)
AA (- DTT)
DHA (+ DTT)
DHA (- DTT)
Time (min)
C
AA
DHA
AA (10 μM)
DHA (300 μM)
Mitochondrial AA (nmol/mg proteins)
Cellular AA (nmol/10^6 cells)
AA or DHA (μM)
D
Mitochondrial AA (nmol/mg proteins)
Cellular AA (nmol/10^6 cells)
DHA (μM)

Figure 9. Mitochondrial accumulation of vitamin C in cells exposed to AA, DHA or the two agents combined. A) The cells were exposed for 15 min to 30 µM AA, or DHA, either alone or combined, and finally analyzed for vitamin C accumulation (inset) or processed for the isolation of the mitochondrial fraction prior to vitamin C analysis (main graph). Results represent the means ± SD calculated from at least 3 separate experiments. *P < 0.001 as compared to the sample exposed to AA (first bar) B) The cells were first exposed for increasing time intervals to 30 µM AA, or DHA, and then processed for vitamin C analysis, with or without addition of 10 mM DTT to the lysates. Results represent the means ± SD calculated from at least 3 separate experiments. C) The cells were exposed for 15 min to increasing concentrations of AA, or DHA, and then processed for the isolation of the mitochondrial fraction prior to vitamin C analysis (main graph). The inset shows the amount of vitamin C accumulated by the cells after exposure to 10 µM AA or 300 µM DHA. Results represent the means ± SD calculated from at least 3 separate experiments. D) Vitamin C accumulation in the mitochondria of cells exposed for 15 min to 30 µM AA and increasing concentrations of DHA (main graph). The inset shows the results of similar experiments in which the vitamin C content was estimated in total cell extracts (○). For comparison, vitamin C content after exposure to DHA alone is also reported (●). Results represent the means ± SD calculated from at least 3 separate experiments. *P < 0.001, as compared to exposure to AA alone (two-way ANOVA followed by Bonferroni's test) [66].

The results obtained were best described by a bimodal curve, with a fast kinetic observed at DHA concentrations < 3 μM, and a remarkably slower kinetic at greater concentrations.

To investigate the accumulation of vitamin C in isolated mitochondria we performed experiments exposing these organelles to 30 μM AA or DHA. Using radiolabeled AA we obtained surprisingly similar kinetics of uptake (Figure 10A). The 5 min exposure time-point was selected to determine that i) AA transport is sensitive to Na^+ omission and insensitive to Cyt B (Figure 10B), thereby implying the exclusive uptake of the reduced form of the vitamin and ii) the amount of the radioactivity associated with exposure to the mixture ascorbate-oxidase/^{14}C-AA is Na^+-independent and sensitive to Cyt B, and hence entirely resulting from DHA uptake. The results illustrated in Figure 10C provide evidence for an identical, DTT-insensitive accumulation of the vitamin in isolated mitochondria exposed to increasing concentrations of AA and DHA. The notion that AA and DHA are taken up by their specific transporters was assessed as in the above experiments (Figure 10D). The results presented in this section collectively indicate that AA and DHA are efficiently and similarly transported into mitochondria through their respective transporters. In addition, once in the mitochondria, AA is kept in its reduced state and DHA is immediately reduced back to AA. Moreover the mitochondrial AA transporter might be susceptible to DHA-dependent

inhibition, as previously observed in the case of plasma membrane SVCT2 [65].

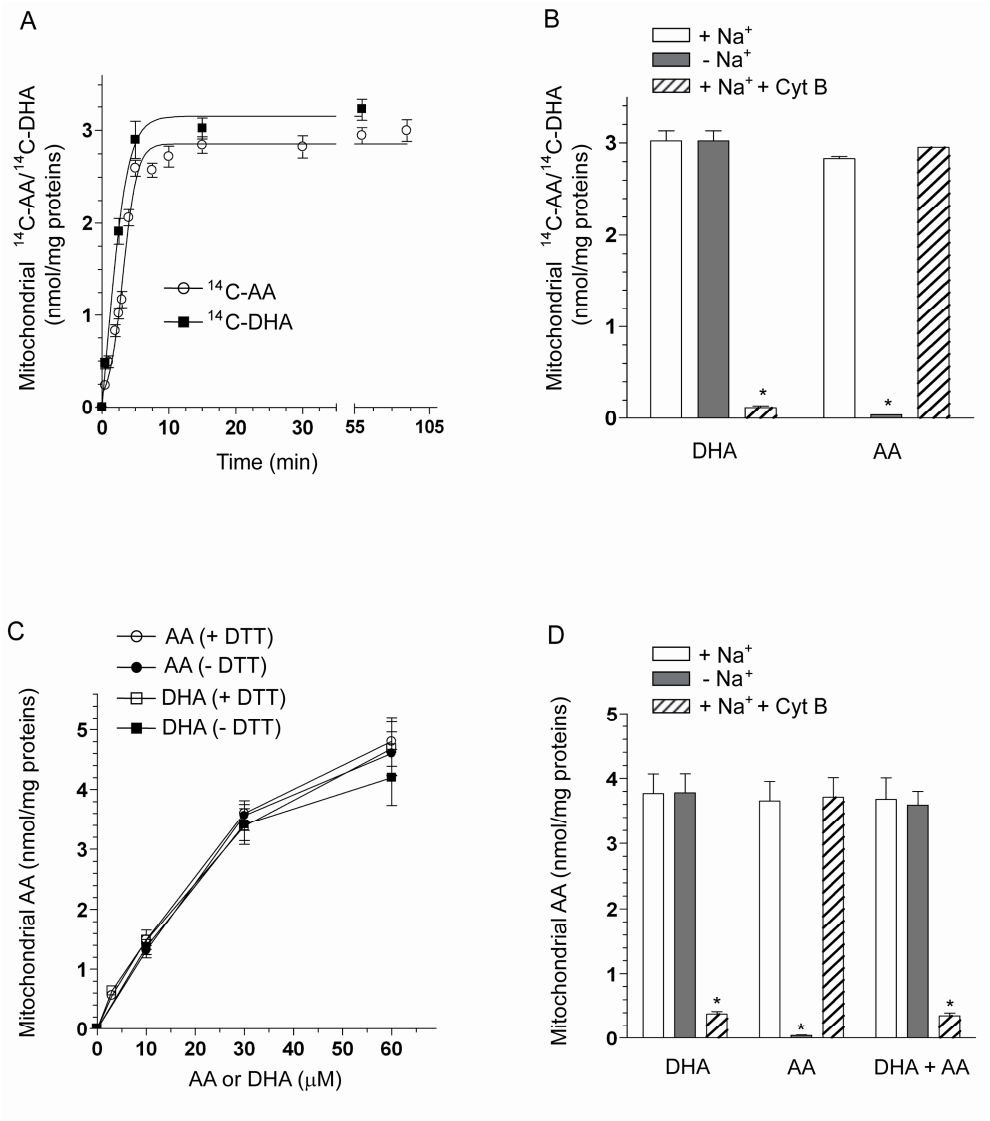

Figure 10. Accumulation of vitamin C in isolated mitochondria from U937 cells exposed to AA, DHA, or the two agents combined. A) Time-dependence of accumulation of vitamin C in isolated mitochondria exposed to 30 µM ^{14}C-AA or 30 µM ^{14}C-DHA (obtained by addition of an excess of ascorbate oxidase to 30 µM ^{14}C-AA). Results represent the means ± SD calculated from 3 separate experiments. B) Isolated mitochondria were exposed to radiolabeled AA, or DHA, both at 30 µM, and then analyzed for vitamin C accumulation. Treatments were performed in MB supplemented with Cytocalasin B (Cyt B), or manipulated to replace sodium-EGTA with sodium-free EGTA. Results represent the means ± SD calculated from at least 3 separate experiments. *P < 0.001, as compared to the first bar of each set (one-way ANOVA followed by Dunnet's test). C) Concentration-dependence of the accumulation of vitamin C in isolated mitochondria exposed for 15 min to AA, or DHA, with or without addition of 10 mM DTT to the lysates prior to HPLC analysis. Results represent the means ± SD calculated from at least 3 separate experiments. D) Isolated mitochondria were exposed to 30 µM AA, or DHA, either alone or combined, and finally analyzed for vitamin C accumulation. Treatments were performed in MB, with the manipulations described in (B). Results represent the means ± SD calculated from at least 3 separate experiments. *P < 0.001, as compared to the first bar of each set (one-way ANOVA followed by Dunnet's test) [66].

We performed experiments using purified mitochondria exposed to 30 μM radiolabelled AA alone or associated with various inhibitors. As indicated in Figure 11A, mitochondrial uptake of the vitamin was suppressed by established inhibitors of plasma membrane SVCT2, as 40 μM pCMB or 200 μM S-Pyr [67, 75], and reduced by a 30 μM concentration of either DHA or quercetin (Figure 11B). We finally performed experiments to determine the reversibility of the effects mediated by DHA on mitochondrial AA transport. The mitochondria were first treated for 15 min with 30 μM DHA, then DHA was removed and the organelles exposed for an additional 15 min to 30 μM AA. As indicated in Figure 11C, AA uptake was very little inhibited in comparison to the condition of concomitant exposure to AA and DHA. In conclusion, our results indicate that SVCT2 is a major physiological transporter in the mitochondria of the cell type employed in this study, and presumably of other cell types characterized by similar AA transporter densities and DHA reductive capacities. In these conditions, DHA is not a likely precursor for mitochondrial vitamin C accumulation. At low intracellular levels, presumably compatible with those achievable "*in vivo*", DHA may rather function as an inhibitor of mitochondrial transport of AA.

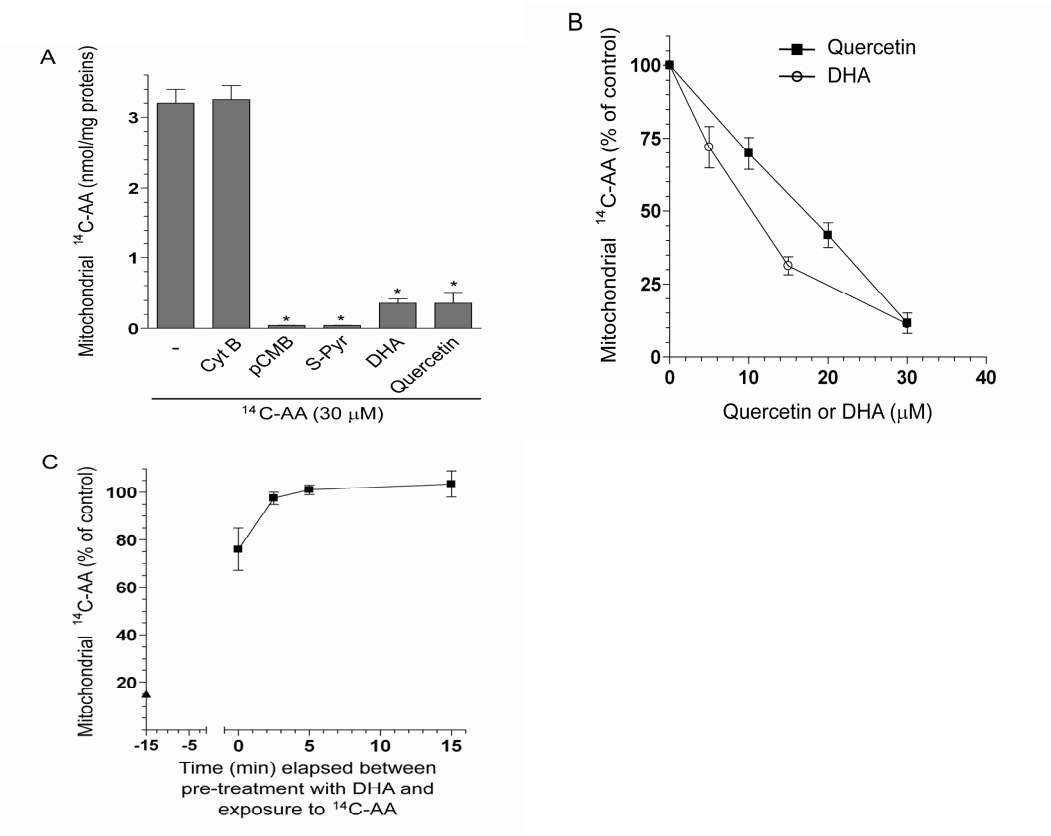

Figure 11. DHA-dependent inhibition of AA uptake in isolated mitochondria from U937 cells. A) Isolated mitochondria were exposed for 15 min to 30 µM ^{14}C-AA alone, or associated with Cyt B (25 µM), pCMB (40 µM), S-Pyr (200 µM), DHA (30 µM) or quercetin (30 µM) and then processed for the assessment of vitamin C accumulation. Results represent the means ± SD calculated from at least 3 separate experiments. *P < 0.001 as compared to the sample exposed to AA (first bar). B) Isolated mitochondria were exposed for 15 min to 30 µM ^{14}C-AA, in the absence or presence of increasing concentrations of either DHA or quercetin, and then processed for the assessment of vitamin C accumulation. Results represent the means ± SD calculated from at least 3 separate experiments. C) Reversibility of the DHA-dependent inhibition of mitochondrial AA transport. Mitochondria were treated for 15 min with 30 µM DHA (time -15 min to 0), centrifuged and then exposed for an additional 15 min to 30 µM ^{14}C-AA,

either immediately (time 0) or after a 2.5, 5 or 15 min incubation in fresh medium. After treatments, the radioactivity associated with the mitochondria was measured as described in the Methods section. For comparison, results obtained under conditions of combined exposure to 30 µM ^{14}C-AA and 30 µM DHA are also included (data in ordinate axis, ▲). Results represent the means ± SD calculated from at least 3 separate experiments [66].

1.2 Characterization of mitochondrial SVCT2 in D-U937 cells.

Early studies performed in our laboratory [74] indicated that the mitochondrial fraction of vitamin C promotes enhancing effects in cells supplemented with otherwise inactive concentrations of peroxynitrite, the coupling product of nitric oxide and superoxide. We more recently demonstrated that superoxide formation takes place at the complex III level in a reaction in which ubisemiquinone serves as an electron donor [68, 70]. Superoxide is then dismutated to H_2O_2, which can either damage the mitochondria or exit these organelles and produce effects in other subcellular compartments, including genomic DNA [68, 69, 71]. A critical event for superoxide formation is represented by the process of peroxynitrite-dependent Ca^{2+} mobilization from the ryanodine receptor and the mitochondrial clearance of the cation [69].Coherently, loss of functional ryanodine receptors leads to a resistance phenotype, as we found in the case of U937 cells differentiated to monocytes [72]. The differentiation process was indeed associated with down-regulated expression of ryanodine receptors and differentiated cells failed to generate mitochondrial superoxide, and became resistant to peroxynitrite toxicity. Human monocytes and macrophages also fail to express the ryanodine receptor and hence display collateral resistance to peroxynitrite [72]. As these cells actively produce peroxynitrite in inflamed tissues, down-regulation of ryanodine receptors appears as an effective strategy to maintain cellular integrity under conditions

associated with the release of large amounts of different oxidants, including peroxynitrite itself. AA is also involved in events regulating cell growth and differentiation in various systems, e.g. *in vitro* differentiation of several mesenchyme-derived cell types [76], and *in vivo* differentiation of connective tissues, such as bone, muscle, and cartilage [77].

Based on these considerations, we investigated the expression and the kinetic characteristics of the cellular and mitochondrial SVCT2 during DMSO-dependent differentiation of promonocytic U937 cells (U-U937) to monocytes (D-U937). The results illustrated in Figure 12A provide evidence for the expression of the two AA transporter isoforms, SVCT1 and 2, at the mRNA level in both U- and D-U937 cells. A significant down-regulation of SVCT2 mRNA during differentiation, with hardly any effect detected in the case of SVCT1 mRNA, was also detected. The observed down-regulation appeared asa very early event of the differentiation process, as it was clearly detectable after only 24h of DMSO exposure (data not shown). Interestingly, the analysis of SVCT2 expression at the protein level (Figure 12B) did not provide evidence of a down-regulation of the transporter at day 4 of DMSO exposure, a likely consequence of the slow turnover of this protein. As expected, we found no difference in terms of SVCT1 protein expression.

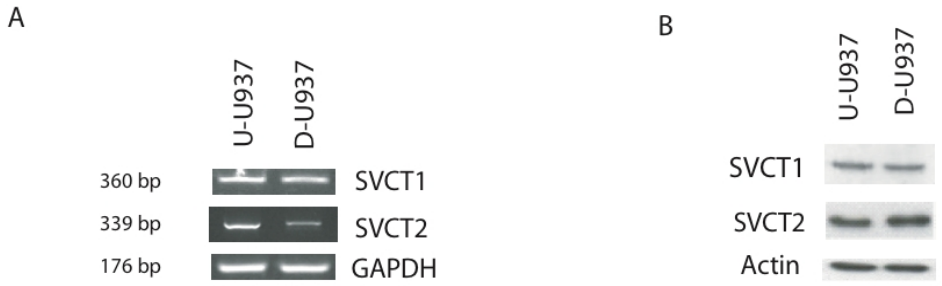

Figure 12. Effects of U937 cells differentiation on SVCTs mRNA and protein expression. A) RT-PCR analysis of SVCT1 and SVCT2 mRNA expression in U-U937 and D-U937 cells; RT-PCR for GAPDH was used as an internal control; B) WB analysis of total cellular lysate of U-U937 and D-U937 cells using anti-SVCT1, anti-SVCT2; anti-actin antibody is used as loading control.

In addition, U-U937 and D-U937 cells were found to take up AA at similar rates(Figure 13). Importantly, under these conditions, AA uptake was entirely dependent on Na^+-AA co-transporter(s). Furthermore, AA transport was suppressed by Na^+ omission, using a buffer in which the ion is replaced by coline, in both the U-U937 and D-U937 cells (not shown).

The above results are therefore indicative of a similar uptake of the reduced form of the vitamin in the two cell types, despite the early suppression of SVCT2 mRNA expression in D-U937 cells.

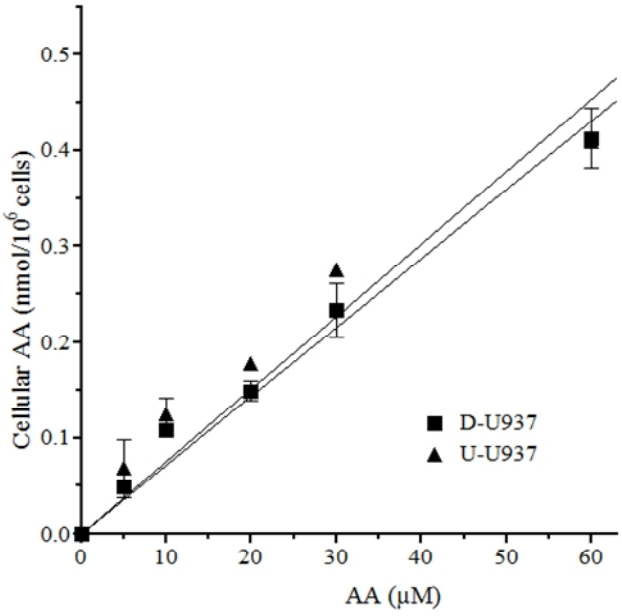

Figure 13. No effect of U937 cells differentiation on the rate of cellular uptake of low concentrations of AA. AA content in U-U937 and D-U937 cells exposed for 15 min to 0-60 μM AA. Results are the means ± SD of at least 3 separate experiments.

In order to characterize mitochondrial AA transport during the differentiation process, U-U937 and D-U937 cells were exposed to increasing concentrations of AA and processed for the isolation of mitochondria for the assessment of their AA content. Interestingly, the results illustrated in Figure 14A provide a clear-cut indication that the fraction of mitochondrial AA is remarkably lower in D-U937 cells. For a correct interpretation of these results, it is important to keep in mind our previous findings indicating that, under similar conditions, intracellular AA is directly taken up by the mitochondria *via* an active Na^+-dependent transporter [44]. An additional information is that mitochondria derived from U-U937 cells only express SVCT2 [44];

these results were reproduced in this study (Figure 14A) and the same lack of anti-SVCT1 immunoreactivity was found in the mitochondria of differentiated cells (Figure 14B).We however obtained the unexpected and apparently contradictory result of enhanced SVCT2 expression in the mitochondria of D-U937 cells. In summary, during the differentiation process of U937 cells, the mitochondrial uptake decreases and this phenomenon is associated with an enhanced expression of the mitochondrial SVCT2.

We extended our AA uptake studies in mitochondria isolated from U-U937 and D-U937 cells. Time-course experiments revealed that the rate of AA uptake was linear in the first 5 min in both cell types (data not shown). Under these conditions, concentration-response studies produced two hyperbolic curves saturating at 30-60 µM AA. Of note, as shown in Figure 14C, we obtained a remarkably lower amount of the vitamin accumulated in isolated mitochondria from D-U937 cells. Analysis of the transport data by the Eadie-Hofstee method produced straight lines (Figure 14D), consistent with the presence of a single functional component on the mitochondria of both cell types. Although apparent Km values were similar (16.05±5.3 µM and 15.5±4.7 µM for U-U937 and D-U937 cell mitochondria, respectively), Vmax values were in fact significantly lower for the D-U937 cells (0.41 ± 0.3 nmol/mg prot/min) *vs* the U-U937 counterpart (0.75 ± 0.8).

The above results provide evidence for a diminution of AA transport in the mitochondria of D-U937 cells uniquely based on a decreased Vmax of mitochondrial SVCT2 transporter, despite enhanced protein expression. While more studies are needed to provide an explanation for these results, it nevertheless appears that SVCT2 immunoreactivity detected in the mitochondria of D-U937 cells is due to an inactive form of the transporter. Recent studies [28], have reported in brain the existence of a shorter SVCT2 isoform of the protein (SVCT2sh), produced by an internal deletion in the mRNA sequence, that, while failing to act as an AA transporter, actually down-regulates the activity of the normal transporter throw a protein-protein interaction. Our results may therefore be compatible with the expression of a SVCT2sh in D-U937 cells, an event associated with a reduced mitochondrial accumulation of AA. We cannot, however, rule out a possible double regulation, at transcriptional and post-transcriptional level, specific for these organelles. There are indeed numerous lines of evidence on the modulation of a protein activity induced by post-translational modifications. I*n silico* analysis of the amino acid sequence revealed the presence of N-glycosylations and phosphorilation sites that can induce conformational modifications of the protein with subsequent modulation of cellular localization and activity [78, 79].

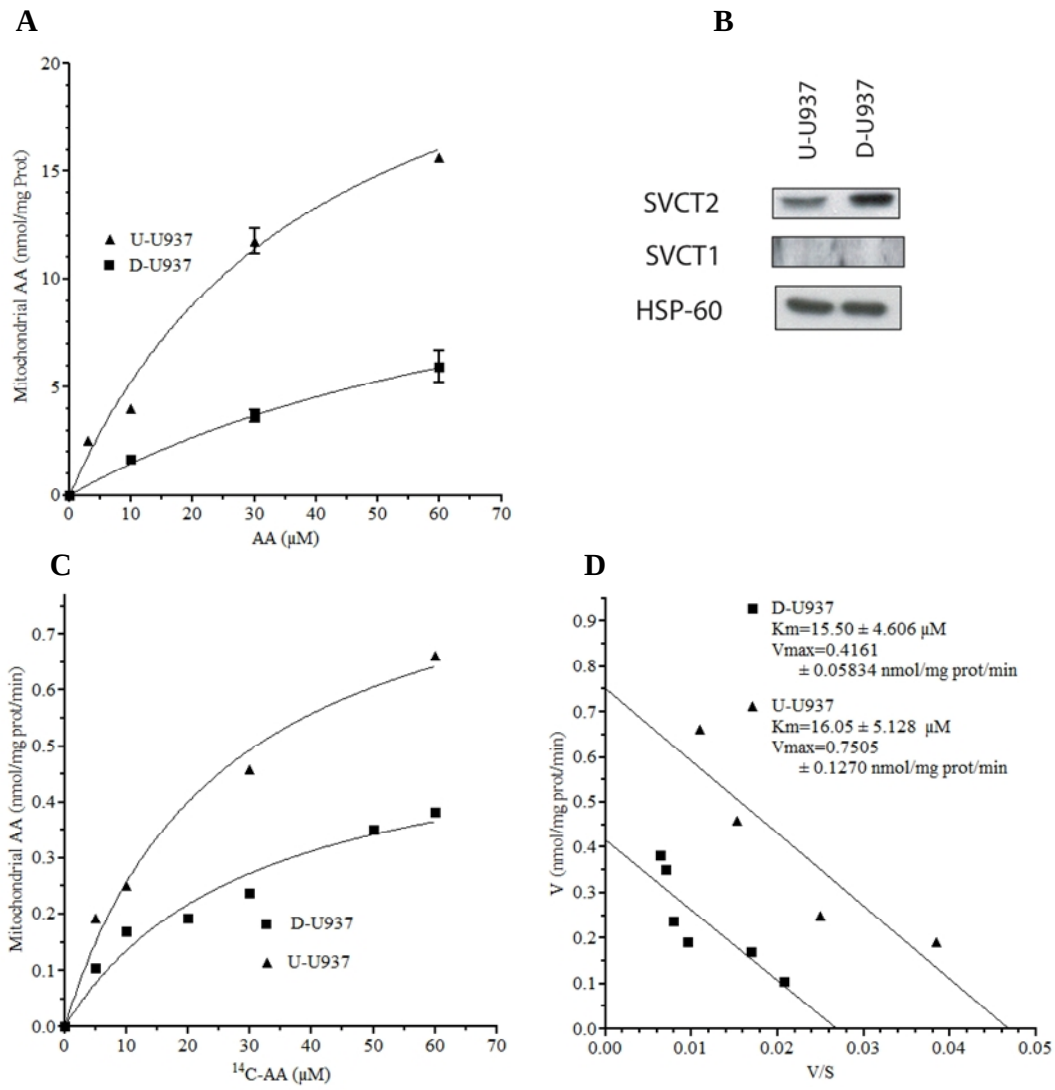

Figure 14.Uptake of AA in the mitochondria of undifferentiated and differentiated U937 cells. A) AA content in mitochondria purified from U-U937 and D-U937 cells pre-exposed to 0-60 μM AA in EB. B) WB analysis of mitochondrial SVCT1 and SVCT2 expression in U-937 and D-U937 cells; HSP-60 protein is used as an internal loading control. Results are the means ± SD of at least 3 separated experiments. C) Mitochondrial AA content in isolated mitochondria from U-U937 and D-U937 cells exposed to 0-60 μM AA. D) Eadie-Hofstee plot of data in C.

The expression of mitochondrial SVCT2 is permissive for a significant accumulation of AA in these organelles; based on this notion, we tested whether such site-specific accumulation -i.e., very high mitochondrial and very low cytosolic concentrations [44]- of the vitamin, was able to selectively affect the impact of toxic substances resulting in mitochondrial dysfunction. For this purpose, we used the toxicity paradigm based on U937 cell exposure to peroxynitrite [69-72].

U-U937 and D-U937 cells were pre-exposed to AA and subsequently treated with 40 uM peroxynitrite, a condition failing to produce significant effects in the absence of additional treatments. Figure 15A shows the results obtained with cells analyzed for their MitoSox Red fluorescence, indicative of mitochondrial $O_2^{-\cdot}$ formation. It can be appreciated that preloading with low concentrations of AA is associated with the selective triggering of peroxynitrite-dependent mitochondrial $O_2^{-\cdot}$ formation in U-U937 cells. In order to obtain a similar response, it was necessary to treat the D-U937 cells with remarkably greater (30-60 μM) concentrations of AA. The results from these experiments were very much similar to, and coherent with, those obtained under identical conditions in cells analyzed for DNA damage with the alkaline halo assay (Figure 15B) or for cytotoxicity (Figure 15C).

Taken together, the results reported above indicate that the process of U937 cell differentiation is accompanied by events resulting in the

gain of a resistance phenotype against the enhancing effects of intra-mitochondrial AA on peroxynitrite-induced superoxide formation, DNA strand scission and cytotoxicity. Since the effects of AA in both the U-U937 and D-U937 cells were similarly affected by the respiratory chain inhibitors (not shown), such a resistance phenotype very likely depends on events associated with the mitochondrial uptake of the vitamin.

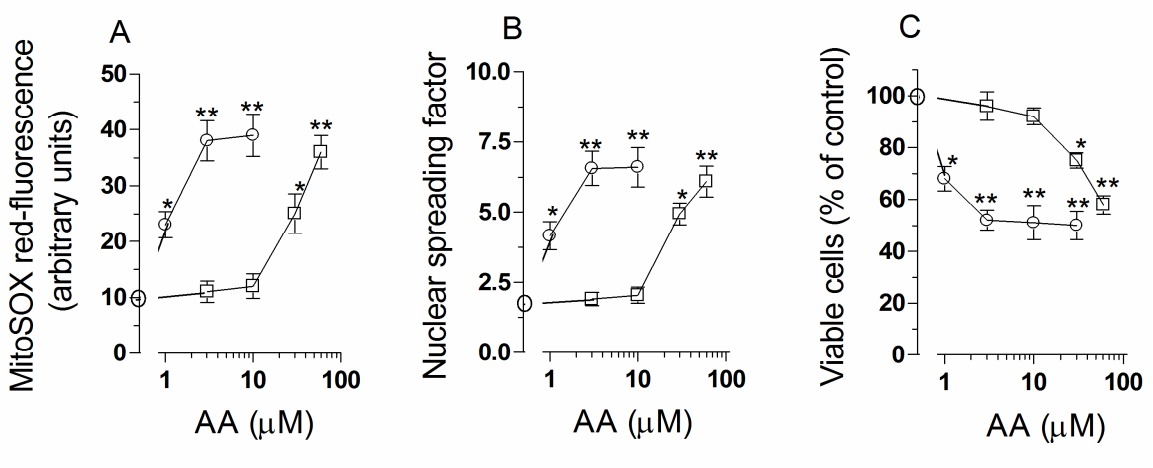

Figure 15. MitoSOX red oxidation, DNA cleavage and toxicity in U-U937 and D-U937 cells exposed to AA and low concentrations of peroxynitrite. U-U937 (circles) or D-U937 (squares) cells were exposed for 15 min to increasing concentrations of AA (0-60 μM) and subsequently incubated in fresh saline A with 40 μM peroxynitrite. MitoSOX red-fluorescence (A), DNA damage (B) and toxicity (C) were determined after 10, 30 and 60 min, respectively. Results represent the means ± SD calculated from at least 3 separate experiments. *P < 0.01; **P < 0.001 as compared to untreated cells (two-way ANOVA followed by Bonferroni's test).

2. ASCORBIC ACID TRANSPORT IN THE SKELETAL MUSCLE.

As previously mentioned, the skeletal muscle contains the largest proportion of total body vitamin C [14, 80, 81]. The skeletal muscle also represents a critical site of ROS production [82] and AA likely mitigates the resulting oxidative damage [83] associated with bouts of physical exercise [84] and observed in individuals affected by type 2 diabetes [85]. Several mouse models exist for the study of the effects resulting from decreased levels of AA *in vivo*. Knockout mice have been generated to study global AA deficits due to lack of AA synthesis (gulo (−/−) [86], and for tissue specific decreases due to knockout of the two AA transporters SVCT2(−/−) [87] and SVCT1(−/−) [30]. SVCT2(−/−) do not survive post birth and show severe hemorrhage in brain accompanying almost undetectable AA levels in SVCT2-dependent organs [86, 87].

Proliferation and differentiation represent mutually exclusive and closely related cellular processes, placed under the control of specific categories of regulatory genes [88, 89]. The antagonism between these processes becomes apparent during development, when many cell types differentiate following irreversible cell cycle arrest. The counterpart of this situation is found instead in cancer cells, in which uncontrolled proliferation is associated with the loss of typical characteristics of cellular terminal differentiation [87-90].The skeletal muscle C2C12 cell line has been widely used in experiments

investigating specific changes occurring in differentiating skeletal muscle cells. In this cellular model, the transition from a myoblast precursor (Mb) to a multi nucleate fiber is finely regulated by the expression of specific genes, accompanied by considerable changes in the synthesis of proteins and morphological changes [62, 88, 91-93]. The C2C12 cells can be maintained in their proliferative state when grown in a medium containing high concentrations of nutrients (10 % FBS); to induce terminal differentiation, Mb are transferred to medium containing low concentrations of nutrients (1% FBS). Under these culture conditions MyoD activity is down-regulated and Mb exit the cell cycle, orient themselves and acquire the myogenic phenotype of mononuclear myocytes; the myocytes fuse and give rise to multinucleated myotubes (Mt). In parallel with these events, the expression of specific genes of terminal differentiation is induced [62, 88, 91-93].C2C12 cells are characterized by an efficient system of vitamin C uptake, represented by SVCT2 and GLUTs for AA and DHA transport, respectively. DHA, once taken up the cells, is then rapidly reduced back to AA [83]. Some studies have shown that the expression of SVCT2 in muscle cells is regulated both at the transcriptional level and translational [29, 78, 94]. Low et al. [95] have shown that, in the muscle cells of chicken embryos, the transport of vitamin C is a positive modulator, since the expression of SVCT2 protein increases during the differentiation from Mb to Mt.

On the basis of our previous results [44, 66], we employed the C2C12 cells to investigate the expression of mitochondrial SVCT2 during differentiation of Mb to Mt. Figure 16 shows the characterization of undifferentiated (Mb) and differentiated C2C12 cells(Mt), with the remarkable morphological changes associated with the expression of markers of the myogenic process[22]. Results reported in Figure 17are indicative of SVCT2 expression at the mRNA and protein levels, with same apparent increase detected in SVCT2 protein of Mt. There was no evidence of SVCT1 expression in Mb and Mt.

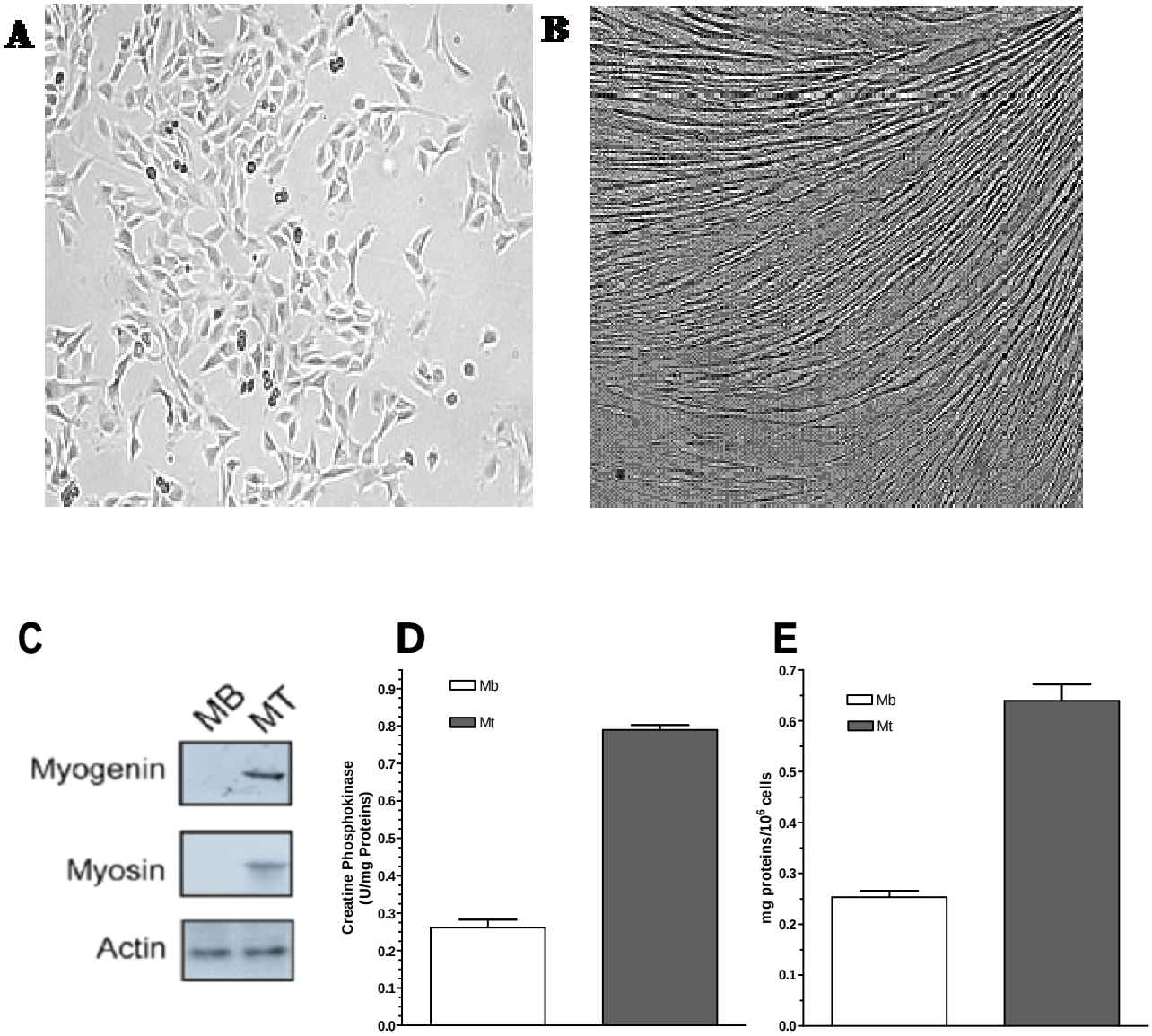

Figure 16. C2C12 Mb and Mt. Representative photographs of Mb (A) and Mt (B). (C) Western blot analysis for myogenin and myosin in Mb and Mt. Actin was used as a loading control. (D) Creatine phosphokinase (CPK) activity of Mb and Mt. (E) Protein content of Mb and Mt. Results are the means ± SD of at least three separate experiments.

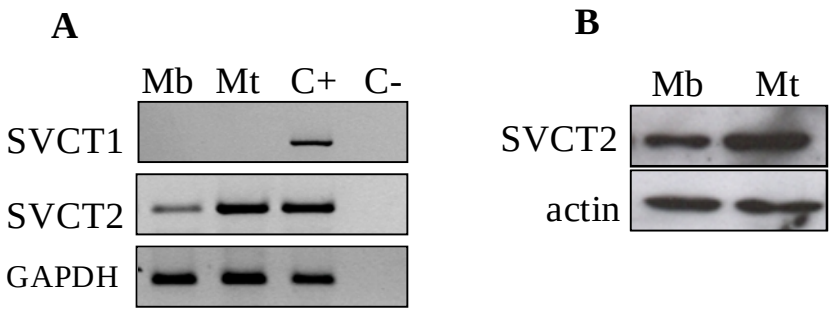

Figure 17.SVCT1 and 2 expression in C2C12 Mb and Mt. A) RT-PCR analysis of SVCT1 and SVCT2 expression in C2C12 Mb and Mt. Total RNA was reverse-transcribed and amplified with SVCT1 or SVCT2 primers. Amplification of the GAPDH is used as internal control. U937 cells were used as positive control for SVCT1 and SVCT2 expression (C+). C- is the reaction mix without template. B) Western blot analysis using antibodies against SVCT2 in C2C12 Mb and Mt. Actin is used as internal loading control. The blot shown is representative of at least 3 separate experiments with similar outcomes.

Time course studies revealed similar rates of AA (60μM) transport in Mb and Mt(Figure 18A). We also observed that AA uptake is in both cell types sensitive to sodium omission, sulphinilpyrazone, and to ice-bath temperature (Figure 18B). We then performed dose-response studies for AA (0-60 μM) uptake and obtained results best described by twosimilar hyperbolic curves (Figure 18C). The analysis of the transport data by the Eadie-Hofstee method demonstrated in the two cell types the presence of single high-affinity transporters, with characteristics compatible with the isoform 2 of SVCT (figure 18D).The Km values were 27.60 uM and 27.04 uM for Mb and Mt, respectively. The Vmax values were 0.30 and 0.27 nmol/min/mg prot for Mb and Mt, respectively.

According to these results, it appears that the differentiation processes fails to promote significant changes in SVCT2 plasma membrane expression and activity. Similar results were previously published [22, 96].

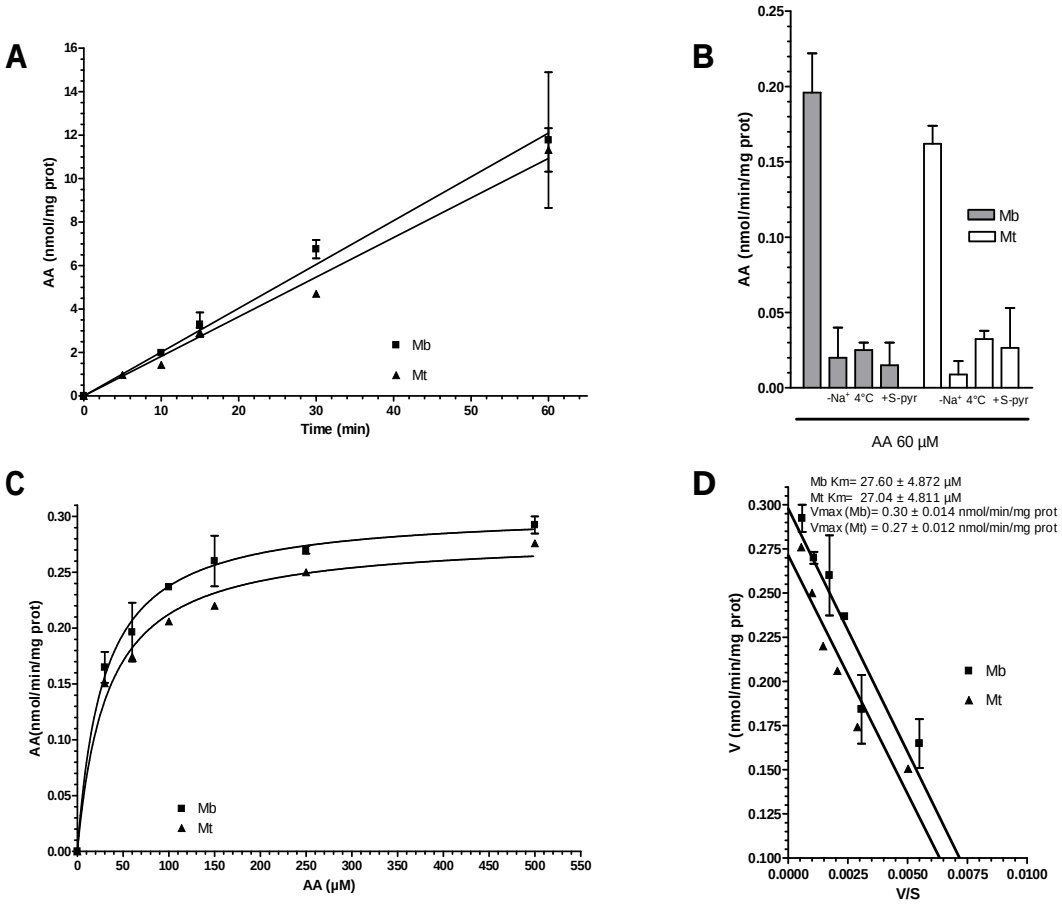

Figure 18. SVCT2-dependent AA uptake in C2C12 Mb and Mt. (A) Time-dependent accumulation of AA (60 µM) in Mb and Mt in EB.(B) Temperature and sodium dependence of AA (60 µM) uptake in Mb and Mt. Effect of S-pyr(200 µM) on AA uptake in the two cell types.(C) Dose-dependence of AA uptake in Mb and Mt (D) Eadie-Hofstee plot of the data reported in B. Values are the means of at least three separate experiments.

Wethen moved to mitochondria isolated from Mb and obtained a linear accumulation of the vitamin in the first 5 minutes of incubation (data not shown). The concentration response-curve (Figure 19A) was hyperbolic and approached saturation at AA concentrations greater than 500 μM. Analysis of the transport data by the Eadie–Hofstee method (Figure19B) produced a straight line (r^2=0,90), consistent with the presence of a single functional component, allowing the calculation of an apparent Km of 451.1 ± 63.76 μM and a Vmax of 3.195 ± 0.02 nmol/min/mg prot. These results indicate that the Mb mitochondrial SVCT2 functions with a low-affinity.

In order to provide direct evidence for the expression of SVCT2 in Mb mitochondria, we performed additional experiments based on various approaches.

The Percoll is a colloidal suspension in polivilpirrolidone (PVP) of silica particles (with a diameter of 17 nm) and this isolation of mitochondria with this technique presents two major advantages with respect to the differential centrifugation method (based on a sucrose gradient): (i) Percoll has a low viscosity, that allows a more rapid sedimentation at a reduced centrifugation speed in comparison with sucrose; (ii) Percoll can be prepared in an isotonic solution for maintaining the osmolarity [97-99].

Samples, obtained as described in Material and Methods, were analyzed by Western blot and TEM.

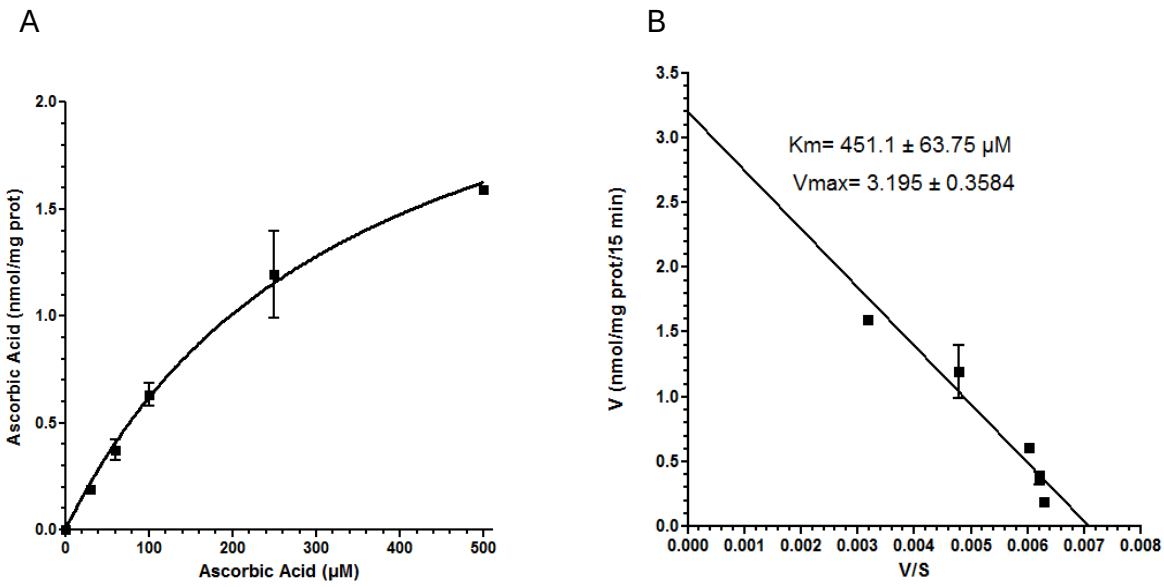

Figure 19.C2C12 Mb mitochondrial SVCT2 functions as a low-affinity AA transporter. A) Concentration-response curve for the transport of AA in isolated mitochondria; B) the Eadie-Hofstee plot of the data reported in (A). Values are the means of at least three separate experiments

As show in Figure 20A, evidence for SVCT2 expression in Mb is restricted to the mitochondrial (Mc and Mp) (positive for cytocrome c and HSP-60) and plasma membrane (PM) (positive for GLUT3) fractions. The Mp fraction was however negative for GLUT3, thereby implying that the mitochondrial immunoreactivity to the anti-SVCT2 antibody was not due to a contamination of the PM fraction. Actin immunoreactivity was present only in the total lysate (tot). Figure 20B is a representative image, obtained with the TEM technique, of the Mp fraction, that shows an enrichment of mitochondria with a fairly good integrity and without strong contaminations due to the other fractions.

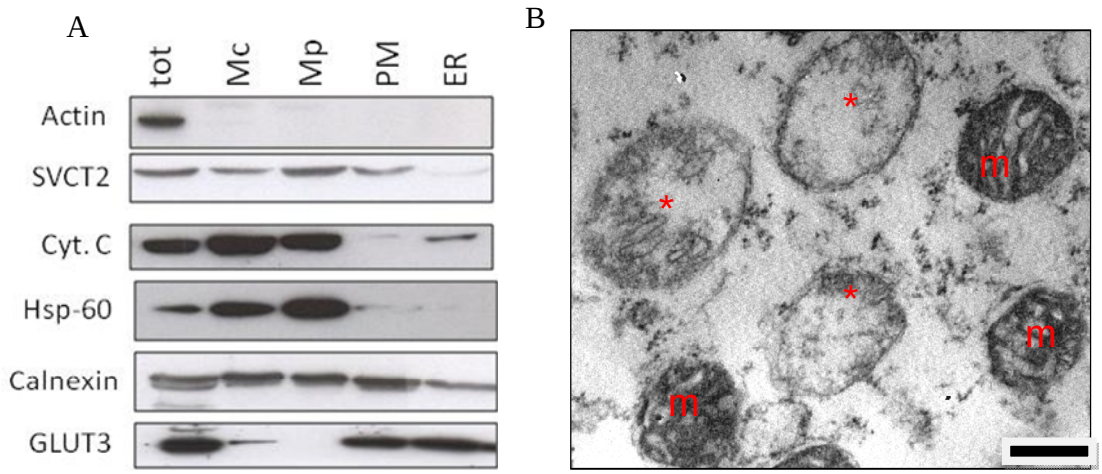

Figure 20. Mitochondrial expression of SVCT2 in C2C12 Mb.

(A) Sub-cellular fractionation and mitochondrial purification. The cells were homogenized and fractionated by differential centrifugation and the Percoll gradient technique. The fractions were separated by SDS-PAGE, transferred to PVDF membranes, and immunodetected with appropriate antibodies. (Tot: total homogenate; Mc: crude mitochondrial fraction; Mp: purified mitochondrial fraction; PM: plasma membrane; ER: endoplasmic reticulum). (B) TEM analysis of pure mitochondrial fraction (Mp). Bar= 2μm. m= mitochondrion, * = empty mitochondrion.

Finally, we performed immunocytochemical analysis of C2C12 Mb labelled with anti-SVCT2 antibody and with a mitochondrial probe, MitoTracker red. Figure 21 (A-D) provides an image of single cells, in which the green identifies the expression of SVCT2 (A), the red the mitochondria (B) and the yellow the co-localized pixels in the overlay image (C). Co-localization analysis was also performed using Image J software, generating a co-localization image in black and white pixels (D). Panel E shows the Pearson's (P) and Manders' (M1 and M2) overlap coefficients. The calculated P coefficient was 0.55 and the M1 coefficient indicated that 70% of the SVCT2 detected overlaps with stained mitochondria.

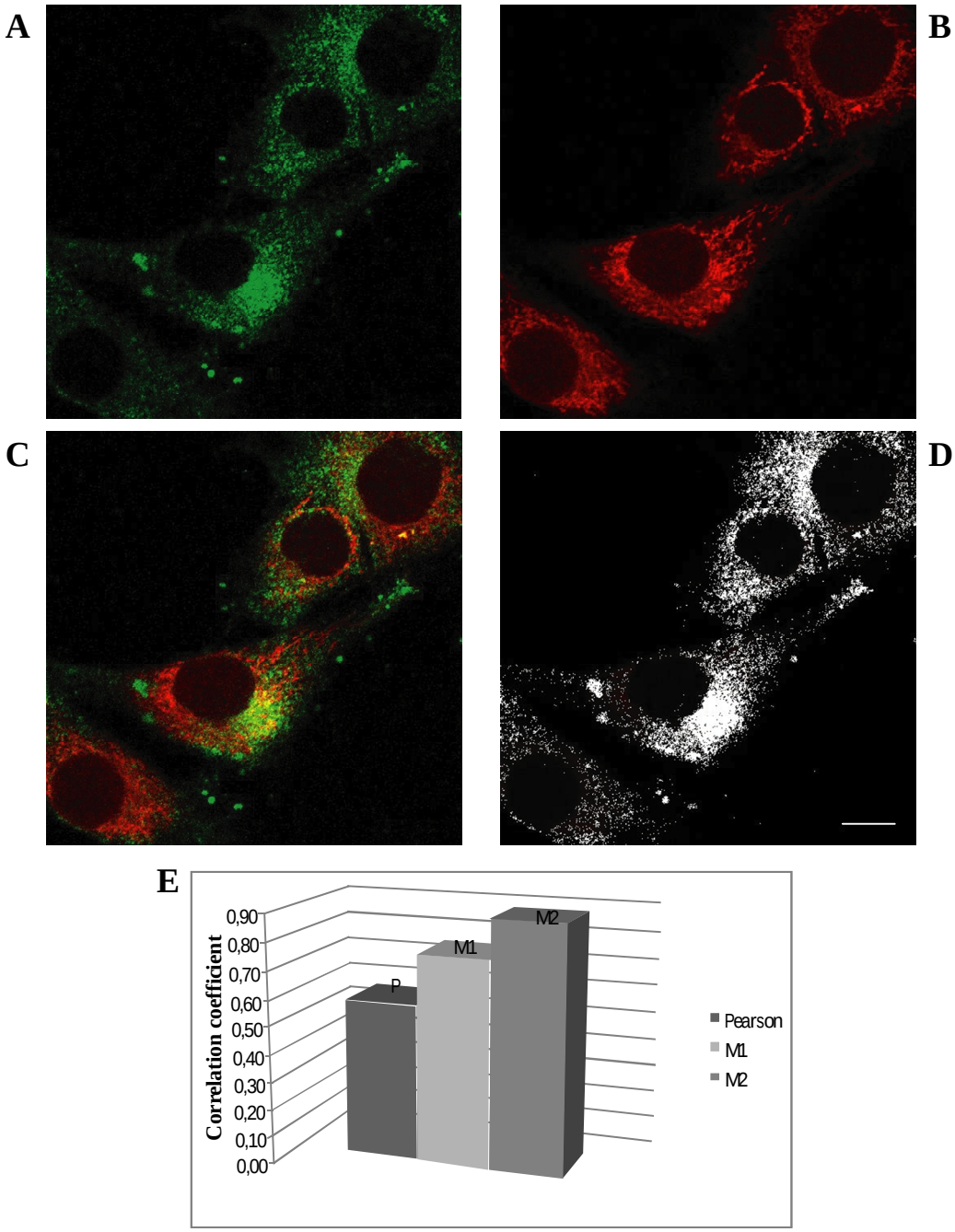

Figure 21. Mitochondrial localization of SVCT2 in C2C12 Mb. (A-D) Representative fluorescence images of cells double stained for SVCT2 (green, A) and mitochondria (MitoTracker Red, B). In the merged image (C) the co-localization appears yellow. (D) Co-localization analysis and quantification performed with Image J software. (E) The Pearson's (P) and Mander's (M1 and M2) overlap coefficients represented as the average of ten images. Bar = 25 μm.

The above experiments provide convincing experimental evidence for the plasma membrane and mitochondrial expression of SVCT2 in C2C12 Mb. In addition, the mitochondrial SVCT2 appears to be characterized by a low affinity for AA.

We then moved to the more complex part of the study, because the problems encountered for the mitochondrial isolation were remarkably more significant when Mt were used in the place of Mb.

The isolation of sub-cellular fractions with a high degree of purity, starting from tissues and mammalian cells, has a great interest since it allows the study and the characterization of specific proteins and organelles. A number of fractionation protocols for the purification of specific organelles has been successfully applied to various cells types but very serious problems have been encountered using the skeletal muscle. This particularly true for the mitochondria of the skeletal muscle, that are characterized by a different architecture in comparison with other tissues [100-102]. In the skeletal muscle, the mitochondria create a three-dimensional network around the sarcomeres [102] and retain functional interactions with the sarcoplasmic reticulum (SR), with lipid droplets and the cytoskeleton. The interaction with the SR is based on a system defined as MAM membranes (membranes associated with mitochondria), very difficult to remove during the process of mitochondria isolation. Indeed MAM membranes generally co-sediment with mitochondria during centrifugation [65]. We therefore performed experiments using

confocal microscopy and TEM analysis in conjunction with WB analysis of the subcellular fractions obtained by Mt using both the differential centrifugation and Percoll gradient techniques, as already described for Mb.

Figure 22A shows that the SVCT2 immunoreactivity is present in the mitochondrial (Mc and Mp), PM and ER fractions. Cytochrome c, the mitochondrial marker, marks weakly the ER fraction, an observation compatible with the possibility that the SVCT2 signal in ER is attributable to a mitochondrial contamination. However, the opposite can also be true because of the persistence of the signal relative to calnexin in both mitochondrial preparations. The existence of a cross-contamination of the mitochondrial and ER fractions was confirmed by results obtained *via* TEM analysis of the Mc fraction. Figure 22C documents the presence of a large number of intact mitochondria along with some membrane fragments,derived from broken mitochondria and/or cellular plasma, and many ribosomes derived from ER. The image shown in panel D, is representative of the Mp fraction, which appears further enriched in mitochondria with however some residual damaged organelle and small fragments of the ER.

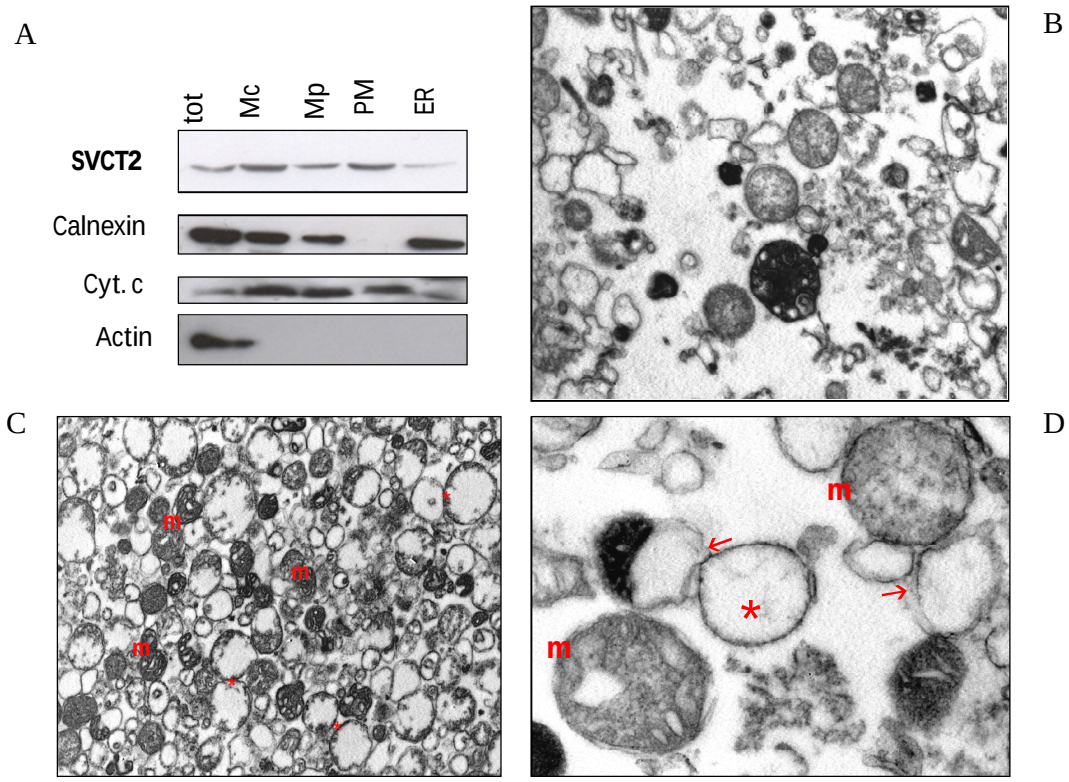

Figure 22. Subcellular localization of SVCT2 in C2C12 Mt.

(A) Subcellular fractionation and mitochondrial purification. The cells were homogenized and fractionated by the differential centrifugation and Percoll gradient techniques. The fractions were separated by SDS-PAGE, transferred to PVDF membranes, and immunodetected with appropriate antibodies. (Tot: total homogenate; Mc: crude mitochondrial fraction; Mp: purified mitochondrial fraction; PM: plasma membrane; ER: endoplasmic reticulum).TEM analysis of (B) total homogenate, (C) crude mitochondrial fraction (Mc) (bar = 10 μm), and (D) purified mitochondrial fraction (Mp) (bar = 2 μm). m = mitochondrion, * = empty mitochondrion,→ = PM and ER pieces.

Finally, we performed an immunocytochemical analysis of C2C12 Mt labelled with anti-SVCT2 antibody and with a mitochondrial probe, MitoTracker red. We observed a heterogeneous expression of the mitochondrial SVCT2 (Figure 23). A more detailed analysis led to the following considerations:

- cells with 1 nucleus are normally characterized by the mitochondrial expression of SVCT2 (signal of co-localization>90%). This is also true in cells presenting evidence of differentiation, i.e., the presence of pseudo-filaments (panels A-B).

- good evidence for a mitochondrial expression of SVCT2 is maintained in Mt with 2 or 3 nuclei (about 75%). In some circumstances, however, an extra-mitochondrial signal was also noted (panels C-D-E-F-G). The arrows indicated the different localization of the green signal.

- Mt with 3 (or more) nuclei generally displayed a weak mitochondrial signal for SVCT2 (panel H). Importantly, however, this conclusion is based on the analysis of a limited number of tri-nucleated cells.

In summary, the results presented in this section suggest that the mitochondrial expression of SVCT2, clearly detected in Mb, is preserved during the differentiation of C2C12 cells-derived Mt. However, the problems encountered during the isolation of mitochondria did not allow a clear-cut demonstration of this notion. At present, we can only suggest that Mt mitochondrial SVCT2 expression decreases at increasing levels of Mt differentiation.

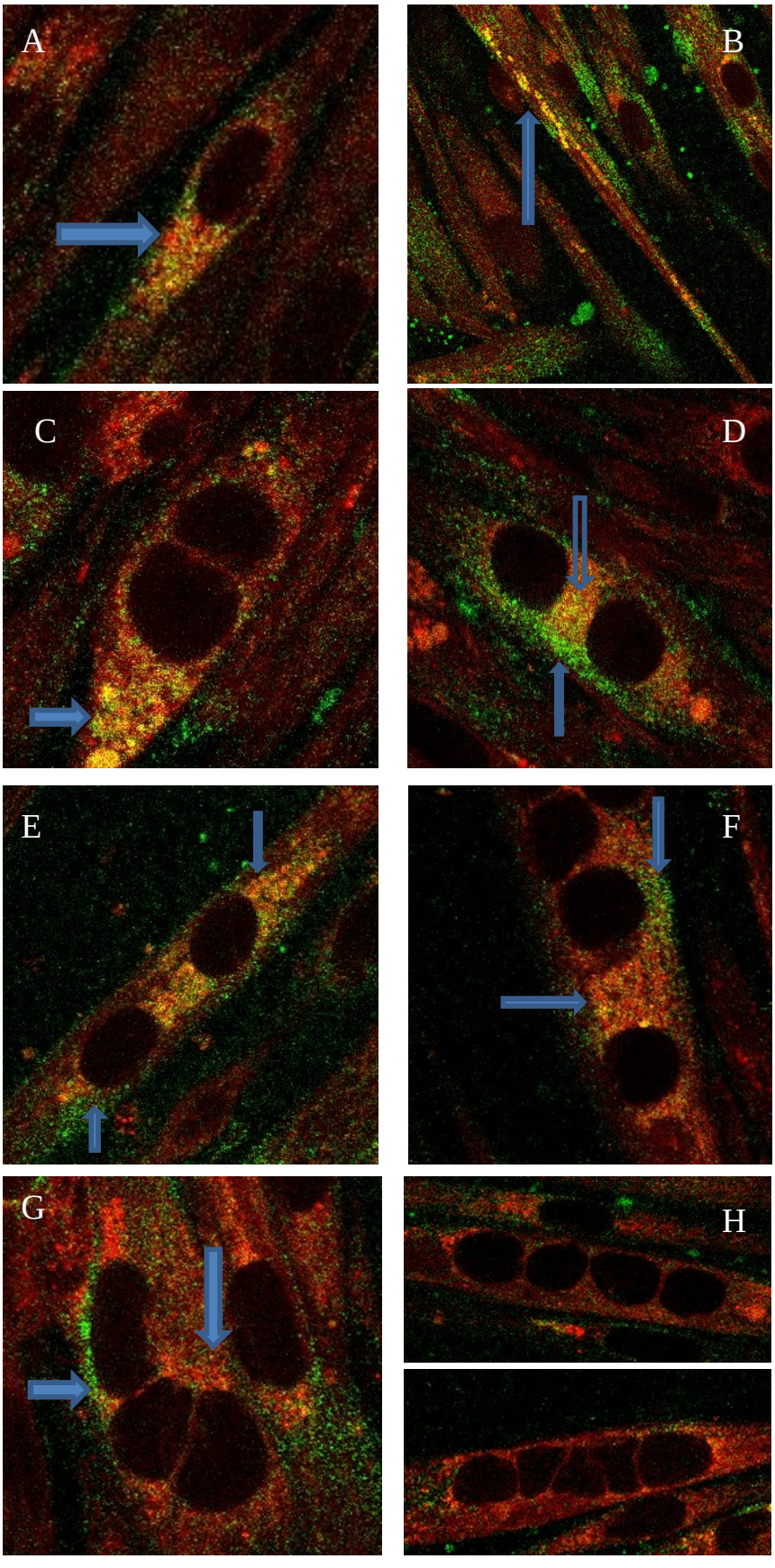
A
B
C
D
E
F
G
H

Figure 23. Mitochondrial localization of SVCT2 in C2C12 Mt. Representative fluorescence images of cells double stained for SVCT2 (green) and mitochondria (MitoTracker Red). In the merged image (A-H) the co-localization appears yellow. Bar = 25 and 50 μm.

We finally performed experiments in the skeletal muscle (*tibialis anterior*) isolated from the hind limbs of CD1 mice. In the initial phase of the *ex vivo* study, we measured the cellular levels of AA. As indicated in Figure 24,we detected approximately 4 nmol/mg of total proteins, in line with the results obtained by other authors [103].

We also made an attempt to measure the mitochondrial fraction of AA and obtained values close to 0.1 nmol/mg mitochondrial proteins. This is indicative of a mitochondrial accumulation of the vitamin since the preparations obtained were surprisingly pure and free of ER contamination. This notion is established by both TEM and WB analyses of the subcellular fractions obtained by the differential centrifugation and Percoll gradient techniques. The TEM images reported in Figure 23 (B-D) provide evidence of intact mitochondria, with well-defined *cristae*, in both Mc (panel C) and Mp (panel D) fractions. WB studies did not provide evidence of a calnexin signal in the mitochondrial preparations and, similarly, there was no evidence of cytochrome c signal in the ER. On the other hand, we observed a very poor expression of SVCT2 transporter isoform in both the total

lysate (tot) and the mitochondrial fractions (Mc and Mp), as shown in Figure 23 A.

These results suggest that the muscle, because at the end of the differentiation pathway, has a more defined structure that makes the mitochondrial separation easier and more efficient. These results, however, are also indicative of poor SVCT2 expression in the muscle, thereby not allowing us to directly ask the question on the in vivo expression of mitochondrial transporter of vitamin C.

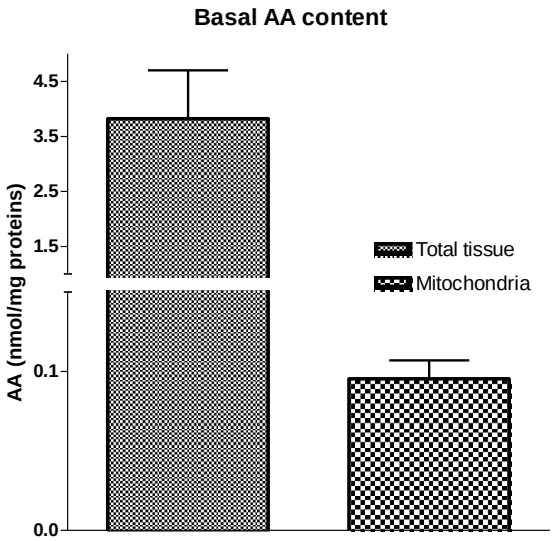

Figure 24. AA content in the skeletal muscle.

Vitamin C content (total and mitochondrial fraction) in the skeletal muscle (*tibialis anterior*) isolated from the hind limbs of CD1 mice.

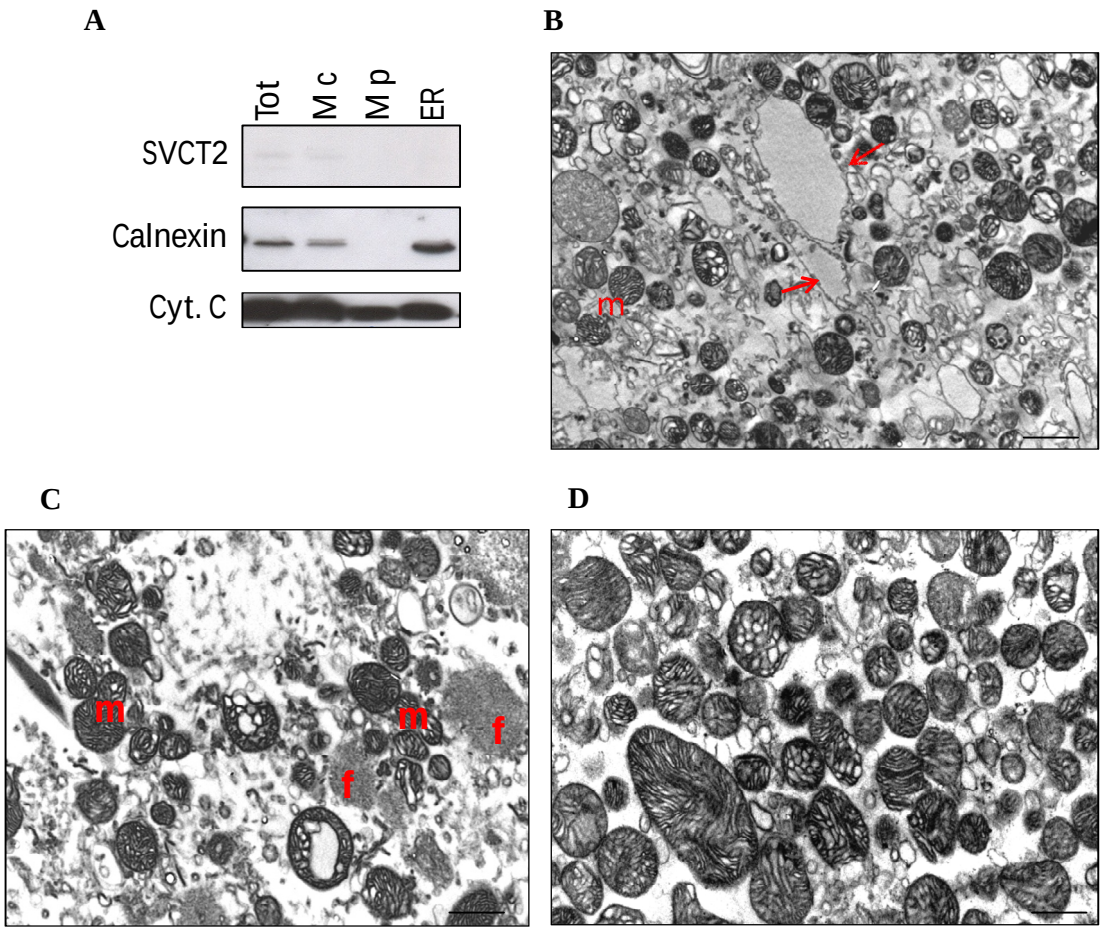

Figure 25. Subcellular fractions of mouse *tibialis anterior* muscle and SVCT2 expression.(A) Subcellular fractionation and mitochondria purification. The tissue was homogenized and fractionated by the Percoll gradient technique and the fractions (Tot: total homogenate; Mc: crude mitochondria; Mp: pure mitochondria; ER: endoplasmic reticulum) were separated by SDS-PAGE, trasferred to PVDF membranes, and immunodetected with appropriate antibodies. (B-D) TEM analysis of total homogenate (B) (bar = 10 mm), crude mitochondria (Mc) (C) (bar = 10 mm), and pure mitochondria (Mp) (D) (bar = 10 mm). m= mitochondrion, -> = plasma membranes, f= muscle fibres.

In conclusion, the results presented in my thesis provide conclusive evidence for the expression and functional activity of mitochondrial SVCT2 in U937 cells. Most importantly, it appears that mitochondrial SVCT2 -unlike the plasma membrane counterpart- is characterized by a high affinity, since this transporter is characterized by a very low requirement for sodium and is virtually calcium independent. We also found that the differentiation of U937 cells to monocytes is accompanied by the loss of expression of SVCT2 mRNA and by the loss of function of mitochondrial SVCT2. This event if probably important to prevent the AA-dependent enhancing effects on peroxynitrite toxicity. Monocyte-derived macrophages indeed actively produce peroxynitrite in the inflamed tissues.

This study also provides evidence for the expression of mitochondrial SVCT2 in C2C12 Mb. In these cells, however, the transporter was found to work with a low affinity. The differentiation of Mb to Mt was accompanied by the formation of a complex network between mitochondria and endoplasmic reticulum, which complicated the process of isolation of mitochondria. Given this premise, we nevertheless conclude that differentiation did not significantly affect the expression/activity of plasma membrane SVCT2 but apparently resulted in a decreased expression of mitochondrial SVCT2. Studies in the mouse skeletal muscle are at present inconclusive since further complicated by the poor overall expression of SVCT2.

BIBLIOGRAPHY

1. Du Juan, Cullen JJ, Buettner GR. "Ascorbic acid: Chemistry, biology and the treatment of cancer". BiochimBiophysActa. 1826: 443–457, 2012.

2. Bogdanski K, Bogdanska H. "Sur la stabilite de l'acide L-dehdroascorbique dans les solutions cbeaqueses". Bull. Acad. Pol. Sci. 3: 41–44, 1955.

3. Figueroa-Méndez R, Rivas-Arancibia S. "Vitamin C in Health and Disease: Its Role in the Metabolism of Cells and Redox State in the Brain".Front Physiol. 23, doi: 10.3389/fphys.2015.00397, 2015.

4. Dhariwal KR, Hartzell WO, Levine M. "Ascorbic acid and dehydroascorbic acid measurements in human plasma and serum". Am J ClinNutr.54:712-7166,1991.

5. Rumsey SC, Knon O, Xu GW, Burant CF, Simpson I, Levine M. "Glucose transporter isoforms GLUT1 and GLUT3 transport dehydroascorbic acid". J BiolChem 272: 18982-9, 1997.

6. Levine M. "New concepts in the biology and biochemistry of ascorbic acid". N Engl J Med. 314:892-902, 1986.

7. Gonzalez CA, Riboli E. "Diet and cancer prevention: contributions from the European Prospective Investigation into Cancer and Nutrition (EPIC) study". Euro. J. Cancer 46: 2555–2562, 2010.

8. Weber P, Bendich A, Schalch W. "Vitamin C and human health—A review of recent data relevant to human requirements". Int. J. Vitam. Nutr. Res. 66: 19–30, 1996.

9. Block G. "Vitamin C and cancer prevention: the epidemiologic evidence". Am. J. Clin. Nutr. 53: 270S–282S, 1991.

10. Loria CM, Klag MJ, Caulfield LE, Whelton PK, "Vitamin C status and mortality in US adults". Am. J. Clin. Nutr. 72: 139–145, 2000.

11. Padayatty SJ, Levine M. "New insights into the physiology and pharmacology of vitamin C". CMAJ 164: 353–355, 2001.

12. Musil F, Zadák Z, Solichová D, Hyšpler R, Kaška M, Sobotka L, Manák J. "Dynamics of antioxidants in patients with acute pancreatitis and in patients operated for colorectal cancer: a clinical study". Nutrition 21: 118–124, 2005.

13. Gruss-Fischer T, Fabian I. "Protection by ascorbic acid from denaturation and re- lease of cytochrome c, alteration of mitochondrial membrane potential and activa- tion of multiple caspases induced by H_2O_2, in human leukemia cells". Biochem. Pharmacol. 63: 1325–1335, 2002.

14. Brown LAS, Jones DP. "The biology of ascorbic acid". In: Cadenas, E., Packer, L. eds. Handbook of Antioxidants. New York: Dekker; 117–154; 1996

15. Vera JC, Rivas CI, Fischbarg J, Golde DW. "Mammalian facilitative hexose transporters mediate the transport of dehydroascorbic acid". Nature 364: 79–82, 1993.

16. Ek A, Ström K, Cotgreave IA. "The uptake of ascorbic acid into human umbilical vein endothelial cells and its effect on oxidant insult". Biochem. Pharmacol. 50: 1339–1346, 1995.

17. Daskalopoulos R, Korcok J, Tao L, Wilson J.X. "Accumulation of intracellular ascorbate from dehydroascorbic acid by astrocytes is decreased after oxidative stress and restored by propofol". Glia 39: 124–132, 2002.

18. Upston JM, Karjalainen A, Bygrave FL, Stocker R. "Efflux of hepatic ascorbate: a potential contributor to the maintenance of plasma vitamin C". Biochem. J. 342: 49–56, 1999.

19. Bánhegyi G, Marcolongo P, Puskás F, Fulceri R, Mandl J, Benedetti A. "Dehydroascorbate and ascorbate transport in rat liver microsomal vesicles". J. Biol. Chem. 30: 2758-2762, 1998.

20. Nardai G, Braun L, Csala M, Mile V, Csermely P, Benedetti A, Mandl J, Banhegyi G. "Protein disulphateisomerase and protein thiol

dependent dehydroascorbate reduction and ascorbate accumulation in the lumen of the endoplasmic reticulum". J. Biol. Chem. 276: 8825–8828, 2001.

21. Tsukaguchi H, Tokui T, Mackenzie B, Berger UV, Chen XZ, Wang Y, Brubaker RF, Hediger MA. "A family of mammalian Na+-dependent L-ascorbic acid transporters". Nature 399:70–75, 1999.

22. Savini I, Rossi A, Pierro C, Avigliano L, Catani MV. "SVCT1 and SVCT2: key proteins for vitamin C uptake". Amino Acids 34:347-55, 2008.

23. Szarka A, Balogh T. "In silico aided thoughts on mitochondrial vitamin C transport". J Theor Biol. 21:181-9,2015.

24. Faaland CA, Race JE, Ricken G, Warner FJ, Williams WJ, Holtzman EJ. "Molecular characterization of two novel transporters from human and mouse kidney and from LLC-PK1 cells reveals a novel conserved family that is homologous to bacterial and Aspergillusnucleobase transporters". BiochimBiophysActa. 8: 353-60,1998.

25. Liang WJ, Johnson D, Jarvis SM. "Vitamin C transport systems of mammalian cells". Mol. Membr. Biol. 18: 87-95, 2001.

26. Wang Y, Mackenzie B, Tsukaguchi H, Weremowicz S, Morton CC, Hediger MA. "Human vitamin C (L-ascorbicacid) transporter SVCT1". BiochemBiophys Res Commun.267:488-494, 2000.

27. Bürzle M, Suzuki Y, Ackermann D, Miyazaki H, Maeda N, Clémençon B, Burrier R, Hediger MA. " The sodium-dependentascorbicacidtransporter family SLC23". Mol Aspects Med. 34:436-454, 2013.

28. Lutsenko EA, Carcamo JM, Golde DW. "A human sodium-dependent vitamin C transporter 2 isoform acts as a dominant-negative inhibitor of ascorbic acid transport". Mol Cell Biol. 24: 3150-6,2004.

29. Biondi C, Pavan B, Dalpiaz A, Medici S, Lunghi L, Vesce F. "Expression and characterization of vitamin C transporter in the human trophoblast cell line HTR-8/SVneo: effect of steroids, flavonoids and NSAIDs". Mol Hum Reprod 13: 77–83, 2007.

30. Corpe CP, Tu H, Eck P, Wang J, Faulhaber-Walter R, Schnermann J, Margolis S, Padayatty S, Sun H, Wang Y, Nussbaum RL, Espey MG, Levine M. "Vitamin C transporter Slc23a1 links renal reabsorption, vitamin C tissue accumulation, and perinatal survival in mice". J Clin Invest. 120: 1069–1083, 2010.

31. Godoy A, Ormazabal V, Moraga-Cid G, Zuniga FA, Sotomayor P, Barra V, Vasquez O, Montecinos V, Mardones L, Guzman C, Villagran M, Aguayo LG, Onate SA, Reyes AM, Carcamo JG, Rivas CI, Vera JC. "Mechanistic insights and functional determinants of the transport cycle of the ascorbic acid transporter SVCT2. Activation by sodium and absolute dependence on bivalent cations". J BiolChem 282: 615-624, 2007.

32. Mackenzie B, Illing AC, Hediger MA. "Transport model of the human Na+-coupled L-ascorbic acid (vitamin C) transporter SVCT1". Am J Physiol Cell Physiol. 294:C451-9, 2008.

33. Rajan DP, Huang W, Dutta B, Devoe LD, Leibach FH, Ganapathy V, Prasad PD. "Human placental sodium-dependent vitamin C transporter (SVCT2): molecular cloning and transport function". BiochemBiophys Res Commun.3: 762-768, 1999.

34. Clark AG, Rohrbaugh AL, Otterness I, Kraus VB. " The effects of ascorbic acid on cartilage metabolism in guinea pig articular cartilage explants". Matrix Biol. 21:175-184, 2002.

35. Corti A, Casini AF, Pompella A. "Cellular pathways for transport and efflux of ascorbate and dehydroascorbate". Arch BiochemBiophys 500: 107-115, 2010.

36. Acuña-Castroviejo D, Martín M, Macías M, Escames G, León J, Khaldy H, Reiter RJ. "Melatonin, mitochondria, and cellular bioenergetics". J Pineal Res. 302: 65-74, 2001.

37. Mitchell P. "Chemiosmotic coupling in oxidative and photosynthetic phosphorylation". Biol Rev CambPhilos Soc. 41: 445-502, 1966.

38. Li X, Cobb CE, Hill KE, Burk RF, May JM. "Mitochondrial uptake and recycling of ascorbic acid". Arch. Biochem. Biophys. 387:143–153, 2001.

39. KC S, Cárcamo JM, Golde DW. "Vitamin C enters mitochondria via facilitative glucose transporter 1 (Glut1) and confers mitochondrial protection against oxidative injury". FASEB J. 19: 1657–1667, 2005.

40. Lee YC, Huang HY, Chang CJ, Cheng CH, Chen YT. "Mitochondrial GLUT10 facilitates dehydroascorbic acid import and protects cells against oxidative stress: mechanistic insight into arterial tortuosity syndrome". Hum Mol Genet. 19: 3721-3733, 2010.

41. Levine M, Padayatty SJ, Espey MG. " Vitamin C: a concentration-function approach yields pharmacology and therapeutic discoveries". Adv. Nutr. 2: 78–88, 2011.

42. Carr AC, Bozonet SM, Pullar JM, Simcock JW, Vissers MC. "Human skeletal muscle ascorbate is highly responsive to changes in vitamin C intake and plasma concentrations". Am. J. Clin. Nutr. 97: 800–807, 2013.

43. Kaufman RJ, Malhotra JD. " Calcium trafficking integrates endoplasmic reticulum function with mitochondrial bioenergetics". Biochim. Biophys. Acta, 1843: 2233–2239, 2014.

44. Azzolini C, Fiorani M, Cerioni L, Guidarelli A, Cantoni O. "Sodium-dependenttrasport of ascorbic acid in U937 cellmiochondria". IUBMB life, 65: 149-153, 2013.

45. Muñoz-Montesino C, Roa FJ, Peña E, González M, Sotomayor K,

Inostroza E, Muñoz CA, González I, Maldonado M, Soliz C, Reyes AM, Vera JC, Rivas CI. "Mitochondrial ascorbic acid transport is mediated by a low-affinity form of the sodium-coupled ascorbic acid transporter-2". Free RadicBiol Med. 70:241-54, 2014.

46. Traber MG, Stevens JF. "Vitamins C and E: beneficial effects from a mechanistic perspective". Free Radic. Biol. Med. 51: 1000-1013, 2011.

47. Frei B, England L,. Ames BN. "Ascorbate is an outstanding antioxidant in human blood plasma". Proc. Natl. Acad. Sci. USA 86: 6377-6381, 1989.

48. Halliwell B. "Vitamin C: antioxidant or pro-oxidant in vivo?". Free Radic. Res. 25: 439-454, 1996.

49. Verrax J, Cadrobbi C, Marques C, Taper H, Habraken Y. "Ascorbate potentiates the cytotoxicity of menadione leading to an oxidative stress that kills cancer cells by a non-apoptotic caspase-3 independent form of cell death". Apoptosis 9: 223-233, 2004.

50. Duarte TL , Jones GD. "Vitamin C modulation of H_2O_2-induced damage and iron homeostasis in human cells". Free Radic. Biol. Med. 43: 1165-1175, 2007.

51. Fiorani M, Azzolini C, Cerioni L, Guidarelli A, Cantoni O. "Superoxide dictates the mode of U937 cell ascorbic acid uptake and prevents the enhancing effects of the vitamin to otherwise nontoxic levels of reactive oxygen/nitrogen species". J. Nutr. Biochem. 24: 467-474, 2013.

52. Guidarelli A, Cerioni L, Fiorani M, Cantoni O. "Differentiation-associated loss of ryanodine receptors: a strategy adopted by monocytes/macrophages to prevent the DNA single-strand breakage induced by peroxynitrite". J. Immunol. 183: 4449-4457, 2009.

53. Koziel K, Lebiedzinska M, Szabadkai G, Onopiuk M, Brutkowski W, Wierzbicka K, Wilczynski G, Pinton P, Duszynski J, Zablocki K,

Wieckowski MR. "Plasma membrane associated membranes (PAM) from Jurkat cells contain STIM1 protein is PAM involved in the capacitative calcium entry?", Int. J. Biochem. Cell. Biol. 41: 2440-2449, 2009.

54. Frezza C, Cipolat S, Scorrano L. "Organelle isolation: functional mitochondria from mouse liver, muscle and cultured fibroblasts". Nat. Protoc. 2: 287-295, 2007.

55. Savini I, Duflot S, Avigliano L. "Dehydroascorbic acid uptake in human keratinocyte cell line (HaCat) is glutathione independent". Biochem. J. 345: 665-672, 2000.

56. Cantoni O, Tommasini I, Cerioni L. "The arachidonate-dependent survival signaling preventing toxicity in monocytes/macrophages exposed to peroxynitrite". Methods Enzymol., 441: 73-82, 2008.

57. Burattini S, Battistelli M, Codenotti S, Falcieri E, Fanzani A, Salucci S. "Melatonin action in tumor skeletal muscle cells: an ultrastructural study". Acta Histochem. 118: 278-28, 2016.

58. Cantoni O, Guidarelli A. "Indirect mechanisms of DNA strand scission by peroxynitrite". Methods Enzymol. 440: 11-120, 2008.

59. Fiorani M, Azzolini C, Cerioni L, Scotti M, Guidarelli A, Ciacci C, Cantoni O. "The mitochondrial transporter of ascorbic acid functions with high affinity in the presence of low millimolar concentrations of sodium and in the absence of calcium and magnesium". Biochim. Biophysic. Acta 1848: 1393–1401, 2015.

60. Castro M, Caprile T, Astuya A, Millan C, Reinicke K, Vera JC, Vasquez O, Aguayo LG, Nualart F. "High-affinity sodium-vitamin C co-transporters (SVCT) expression in embryonic mouse neurons", J. Neurochem. 78: 815–823, 2001.

61. Portugal CC, da Encarnacao TG, Socodato R, Moreira SR, Brudzewsky D, Ambrosio AF, Paes-de-Carvalho R. " Nitric oxide modulates

sodium vitamin C transporter 2 (SVCT-2) protein expression via protein kinase G (PKG) and nuclear factor-kappaB (NF-kappaB)". J. Biol. Chem. 287: 3860–3872, 2012.

62. Sartorelli V, Caretti G. "Mechanisms underlying the transcriptional regulation of skeletal myogenesis". CurrOpin Genet Dev. 15: 528-35, 2005.

63. Ormazabal V, Zuniga FA, Escobar E, Aylwin C, Salas-Burgos A, Godoy A, Reyes AM, Vera JC, Rivas CI. " Histidine residues in the Na+-coupled ascorbic acid transporter-2 (SVCT2) are central regulators of SVCT2 function, modulating pH sensitivity, transporter kinetics, Na+ cooperativity, conformational stability, and subcellular localization, J Biol Chem 285 : 36471-36485, 2010.

64. Guidarelli A, Fiorani M, Azzolini C, Cerioni L, Scotti M, Cantoni O. "U937 cell apoptosis induced by arsenite is prevented by low concentrations of mitochondrial ascorbic acid with hardly any effect mediated by the cytosolic fraction of the vitamin". Biofactors. 41: 101-10, 2015.

65. Fiorani M, Azzolini C, Guidarelli A, Cerioni L, Cantoni O. "A novel biological role of dehydroascorbic acid: Inhibition of Na^+-dependent transport of ascorbic acid". Pharmacol. Res. 84: 12-17, 2014.

66. Fiorani M, Azzolini C, Guidarelli A, Cerioni L, Scotti M, Cantoni O. "Intracellular dehydroascorbic acid inhibits SVCT2-dependent transport of ascorbic acid in mitochondria". Pharmacol. Res. 99: 289-295, 2015.

67. May JM, Qu Z. "Redox regulation of ascorbic acid transport: Role of transporter and intracellular sulfhydryls". Biofactors 20: 199-211, 2004.

68. Guidarelli A, Tommasini I, Fiorani M, Cantoni O. "Essential role of the mitochondrial respiratory chain in peroxynitrite-induced strand scission of genomic DNA, IUBMB Life 50: 195-201, 2000.

69. Guidarelli A, Sciorati C, Clementi E, Cantoni O. "Peroxynitrite mobilizes calcium ions from ryanodine-sensitive stores, a process associated with the mitochondrial accumulation of the cation and the enforced formation of species mediating cleavage of genomic DNA". Free Radic. Biol. Med. 41: 154-164, 2006.

70. Guidarelli A, Cerioni L, Cantoni O. "Inhibition of complex III promotes loss of Ca2+ dependence for mitochondrial superoxide formation and permeability transition evoked by peroxynitrite". J. Cell Science, 120: 1908-1914, 2007.

71. Guidarelli A, Fiorani M, Azzolini C, Cantoni O. "A novel mechanism, uniquely dependent on mitochondrial calcium accumulation, whereby peroxynitrite promotes formation of superoxide/hydrogen peroxide and the ensuing strand scission of genomic DNA". Antiox. Redox Signal., 13: 745-756, 2010.

72. Guidarelli A, Cerioni L, Fiorani M, Cantoni O. "Differentiation-associated loss of ryanodine receptors: a strategy adopted by monocytes/macrophages to prevent the DNA single-strand breakage induced by peroxynitrite". J. Immunol., 183: 4449-4457, 2009.

73. Guidarelli A, Carloni S, Balduini W, Fiorani M, Cantoni O. "Mitochondrial ascorbic acid prevents mitochondrial O2.- formation, an event critical for U937 cell apoptosis induced by arsenite through both autophagic-dependent and independent mechanisms". Biofactors, 42: 190-200, 2016.

74. Guidarelli A, Cerioni L, Fiorani M, Azzolini C, Cantoni O. "Mitochondrial ascorbic acid is responsible for enhanced susceptibility of U937 cells to the toxic effects of peroxynitrite". Biofactors, 40: 236-246, 2014.

75. Qiao H, May JM. "Macrophage differentiation increases expression of the ascorbate transporter (SVCT2)". Free RadicBiol Med 46:1221-1232, 2009.

76. Farquharson C, Berry JL, Mawer EB, Seawright E, Whitehead CC."Ascorbic acid-induced chondrocyte terminal differentiation: the role of the extracellular matrix and 1,25-dihydroxyvitamin D". Eur J Cell Biol. 76:110-8, 1998.

77. Franceschi RT. "The role of ascorbic acid in mesenchymal differentiation". Nutr Rev. 50:65-70, 1992.

78. Wu X, Itoh N, Taniguchi T, Nakanishi T, Tanaka K."Requirement of calcium and phosphate ions in expression of sodium-dependent vitamin C transporter 2 and osteopont in in MC3T3-E1 osteoblastic cells". BiochimBiophysActa 1641: 65–70, 2003.

79. Caprile T, Salazar K, Astuya A, Cisternas P, Silva-Alvarez C, Montecinos H, Millan C, de Los Angeles Garcia M, Nualart F. "The Na+-dependent L-ascorbic acid transporter SVCT2 expressed in brainstem cells, neurons, and neuroblastoma cells is inhibited by flavonoids". J Neurochem 108:563-577,2009.

80. Baker EM, Hodges RE, Hood J, Sauberlich HE, March SC, Canham JE. "Metabolism of 14C- and 3H-labeled L-ascorbic acid in human scurvy". Am. J. Clin. Nutr. 24:444–454, 1971.

81. Schaus R. "The ascorbic acid content of human pituitary, cerebral cortex, heart, and skeletal muscle and its relation to age". Am. J. Clin. Nutr. 5:39–41, 1957.

82. Powers SK,Nelson WB, Hudson MB. "Exercise-induced oxidative stress in humans: cause and consequences". Free Radic. Biol. Med. 51:942–950, 2011.

83. Savini I, Catani MV, Duranti G, Ceci R, Sabatini S, Avigliano R. "Vitamin C homeostasis in skeletalmusclecells". Free RadicBiolMed 38: 898–907, 2005.

84. Davies KJ, Quintanilha AT, Brooks GA, Packer L. "Free radicals and tissue damage produced by exercise". Biochem. Biophys. Res. Commun. 107:1198–1205, 1982.

85. Anderson EJ, Lustig ME, Boyle KE, Woodlief TL, Kane DA, Lin CT, Price 3rd JW, Kang L, Rabinovitch PS, Szeto HH, Houmard JA, Cortright RN, Wasserman DH, Neufer PD. "Mitochondrial H2O2 emission and cellular redox state link excess fat intake to insulin resistance in both 116 rodents and humans". J. Clin. Invest. 119:573–581, 2009.

86. Harrison FE, Meredith ME, Dawes SM, Saskowski JL, May JM. "Low ascorbic acid and increased oxidative stress in gulo(-/-) mice during development". Brain Res. 19, 143-52. doi: 10.1016/j.brainres.2010.06.037

87. Sotiriou S, Gispert S, Cheng J, Wang Y, Chen A, et al. "Ascorbic-acid transporter Slc23a1 is essential for vitamin C transport into the brain and for perinatal survival". Nat. Med. 8: 514–517, 2002.

88. Bentzinger CF, Wang YX, Rudnicki MA. "Building muscle: molecular regulation of myogenesis". Cold Spring HarbPerspect Biol. 4, 2012.

89. Perry RL, Rudnick MA. "Molecular mechanisms regulating myogenic determination and differentiation". Front Biosci 5: 750-67, 2000.

90. Kitzmann M, Fernandez A. "Crosstalk between cell cycle regulators and the myogenic factor MyoD in skeletal myoblasts". Cellular and Molecular Life Sciences. 58: 571-579, 2001.

91. Ferri P, Barbieri E, Burattini S, Guescini M."Expression and subcellular localization of myogenic regulatory factors during the differentiation

of skeletal muscle in C2C12 myoblasts". Journal of Cellular Biochemistry 108: 1302-1317, 2009.

92. Maione R, Amati P. "Interdependence between muscle differentiation and cell-cycle control".Biochim. Biophys. Acta M19-M30, 1997.

93. Sabourin LA. "The molecular regulation of myogenesis". Clin Genet. 57: 16-25, 2000.

94. Fujita I, Hirano J, Itoh N, Nakanishi T, Tanaka K. "Dexamethasone induces sodium-dependant vitamin C transporter in a mouse osteoblastic cell line MC3T3-E1". Br J Nutr 86: 145–149, 2001.

95. Low M, Sandoval D, Morales B, Mualart F, Henriquez JP. "Up-regulation of the vitamin C transporter SVCT2 upon differentiation and depolarization of myotubes". FEBS Lett585 : 390-396, 2010.

96. Savini I, Catani MV, Duranti G, Ceci R, Sabatini S, Avigliano R. "Vitamin C homeostasis in skeletalmusclecells". Free RadicBiolMed 38: 898–907, 2005.

97. Dimauro I, Pearson T, Caporossi D, Jackson MJ. "A simple protocol for the subcellular fractionation of skeletal muscle cells and tissue". BMC Res Notes. 5: 513, 2012.

98. Koziel K, Lebiedzinska M, Szabadkai G, Onopiuk M, Brutkowski W, Wierzbicka K, Wilczynski G, Pinton P, Duszynski J, Zablocki K, Wieckowski MR. "Plasma membrane associated membranes (PAM) from Jurkat cells contain STIM1 protein is PAM involved in the capacitative calcium entry?".Int J Biochem Cell Biol 41: 2440-2449, 2009.

99. Lebiedzinska M, Szabadkai G, Jones AW, Duszynski J, Wieckowski MR. " Interactions betweentheendoplasmicreticulum, mitochondria, plasmamembraneandothersubcellularorganelles". Int J BiochemCellBiol. 41: 1805-16, 2009.

100. BakeevaLE, ChentsovYuS, Skulachev VP. "Mitochondrialframework (reticulummitochondriale) in rat diaphragmmuscle". BiochimBiophys Acta. 501: 349-69, 1978.

101. Kirkwood SP, Munn EA, Brooks GA. "Mitochondrialreticulum in limbskeletalmuscle". Am J Physiol. 251: 395-402, 1986.

102. Ogata T, Yamasaki Y. "Ultra-high-resolution scanning electron microscopy of mitochondria and sarcoplasmic reticulum arrangement in human red, white, and intermediate muscle fibers". Anat Rec. 248:214-23, 1997.

103. Iwama M, Amano A, Shimokado K, Maruyama N, Ishigami A. "Ascorbic acid levels in various tissues, plasma and urine of mice". J Nutr Sci Vitaminol 58: 169-174, 2012.